OBSERVATIONS OF PROPAGATION CHARACTERISTICS OF A WIND DRIVEN SEA

by

Ortwin Hartmut von Zweck

B.A. Northeastern University
(1963)

M.S. Northeastern University

(1965)

Submitted in partial fulfillment
of the requirement for the
degree of Doctor of Philosophy

at the

Massachusetts Institute of Technology

February, 1970

Signature of Author .....

Certified by .....
Thesis Supervisor

Accepted by .....
Chairman, Departmental Committee
on Graduate Students

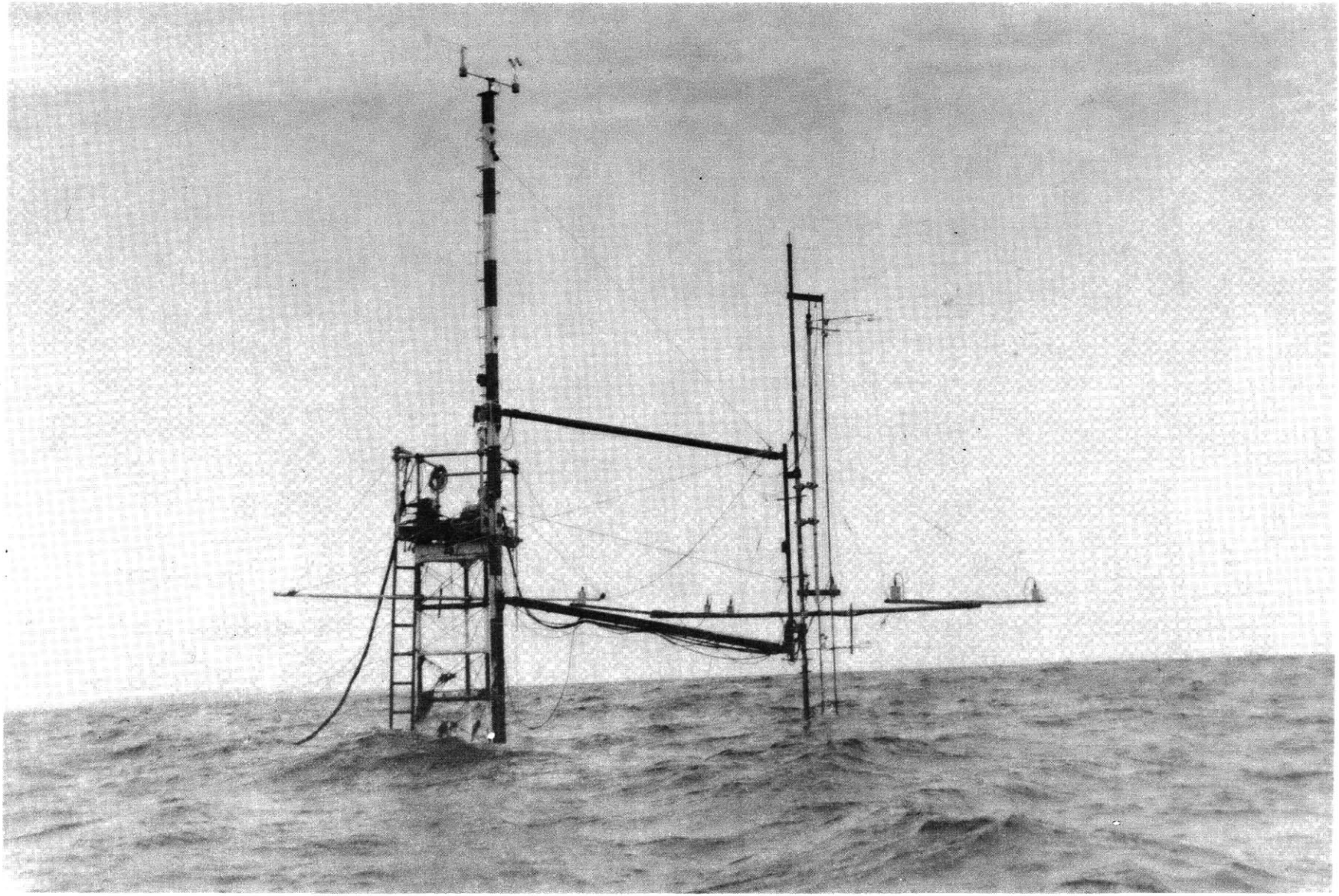

Observations of Propagation

Characteristics of a Wind Driven Sea

Ortwin Hartmut von Zweck

Abstract

The aim of this study was the investigation of propagation characteristics of gravity waves from wave height measurements obtained in the open ocean.

Results of two sets of measurements yielded values of phase speeds equal to and larger than the theoretical phase speeds given for waves of that frequency by the linear dispersion relation.

The observed phase speed excess can be explained by the existence of wave spread and a theoretical angular energy distribution, based on present theories of wave generation, is proposed.

A direct proof of the suggested energy distribution by directional spectral analysis methods performed on sample angular distribution proved to be unsuccessful because of the poor directional spectral resolution obtained for wave gauge array. Comparison of the measured results and the theoretical model of wave spread demanded a knowledge of the stages of wave growth present during data collection, because of the uncertainty of initial conditions this could however not be determined from the wind observation. Spectral growth was therefore analyzed in terms of spectral time series.

An agreement between the wave speeds predicted by the theoretical angular energy distribution and the measured phase speed was found but proof for acceptance or rejection of the suggested angular energy distribution was insufficient.

*

Thesis Supervisor: Erik Mollo-Christensen

Title: Professor of Meteorology

Table of Contents

List of Illustrations

Tables

I. Introduction

One of the obvious ways to experimentally check the resonant theory of wave generation by wind advanced by Phillips (1957) is to compare the predicted bimodal angular energy distribution with directional spectral analysis performed on wave height measurements collected during wave generating conditions. Several approaches for calculating directional spectra have been investigated [Barber (1963), Longuet-Higgins et al (1963), Ford (1967) Hasselman et al (1963)]. Two experimental studies are of interest here, Longuet-Higgins et al (1963) found the directional wave energy spectra by analysing the motion of a free floating buoy. Gilchrist (1966) used the cross-spectral approach by Barber (1963) for wave height data collected by a number of wave gauges arranged in an array. The directional spectra found by these two investigations for wave generating wind conditions appear remarkably similar and both studies essentially equated the widths of the unimodal energy spectra to the resonance angles of the bimodal angular energy distribution predicted by Phillips and found agreement between theory and experimental results.

The present investigation assumes a slightly different point of view. The existence of an angular energy distribution is shown to result in phase speed measurements obtained as a function of frequency for the wave field which exceeds the phase speeds predicted by the

dispersion relation for gravity waves given in Lamb (1932). Agreement between the phase speeds calculated by cross-spectral analysis as shown for example by Laster and Linville (1966), and the angular energy distribution suggested on basis of resonance theory and a wave spread model by Hasselman et al (1963) is sought for a developing wind driven sea.

II. Field Facilities

II.1 Site

The site of the MIT air-sea interaction field work carried out during the summer of 1968 was about 400 feet southeast of the Buzzards Bay Entrance Light Station (BBELS) which marks the location of a shoal at the entrance of Buzzards Bay, Massachusetts. The closest islands are Cuttyhunk, four nautical miles to the east northeast, Martha's Vineyard, nine nautical miles southeast, and Block Island 26 nautical miles to the southwest. The mainland is 6 nautical miles to the north.

Water depth at the site is 19 meters and remains at about 25 meters for a distance of 20 nm in the southwesterly direction. The shoal, which is about 12 meters deep, 1/2 mile wide and 1 1/2 miles long, lies 2 nm from the site in the southwesterly direction. A second 19-meter shoals is about 250 meters from the spar and encompasses the angle between 230° and 330° true. Its width is roughly 200 meters. A chart of the area appears as figure 1.

During the summer the prevailing winds come from the southwest and have a speed of 6-8 meters/sec. On days considered suitable for data collection the wind came from the south to southwest while the swell from the open ocean would be from the south. Shonting (1967) made an extensive survey of the tidal currents encountered at the site. The mean speed of the rotary tide was found to be 14.1 cm/sec with a variance of 29.5 cm^2/sec^2. The maximum current measured was 36.6 cm/sec and mean tidal range is roughly 80-90 cm. Beside the above mentioned study by Shonting the site was used by MIT during the summer of 1967

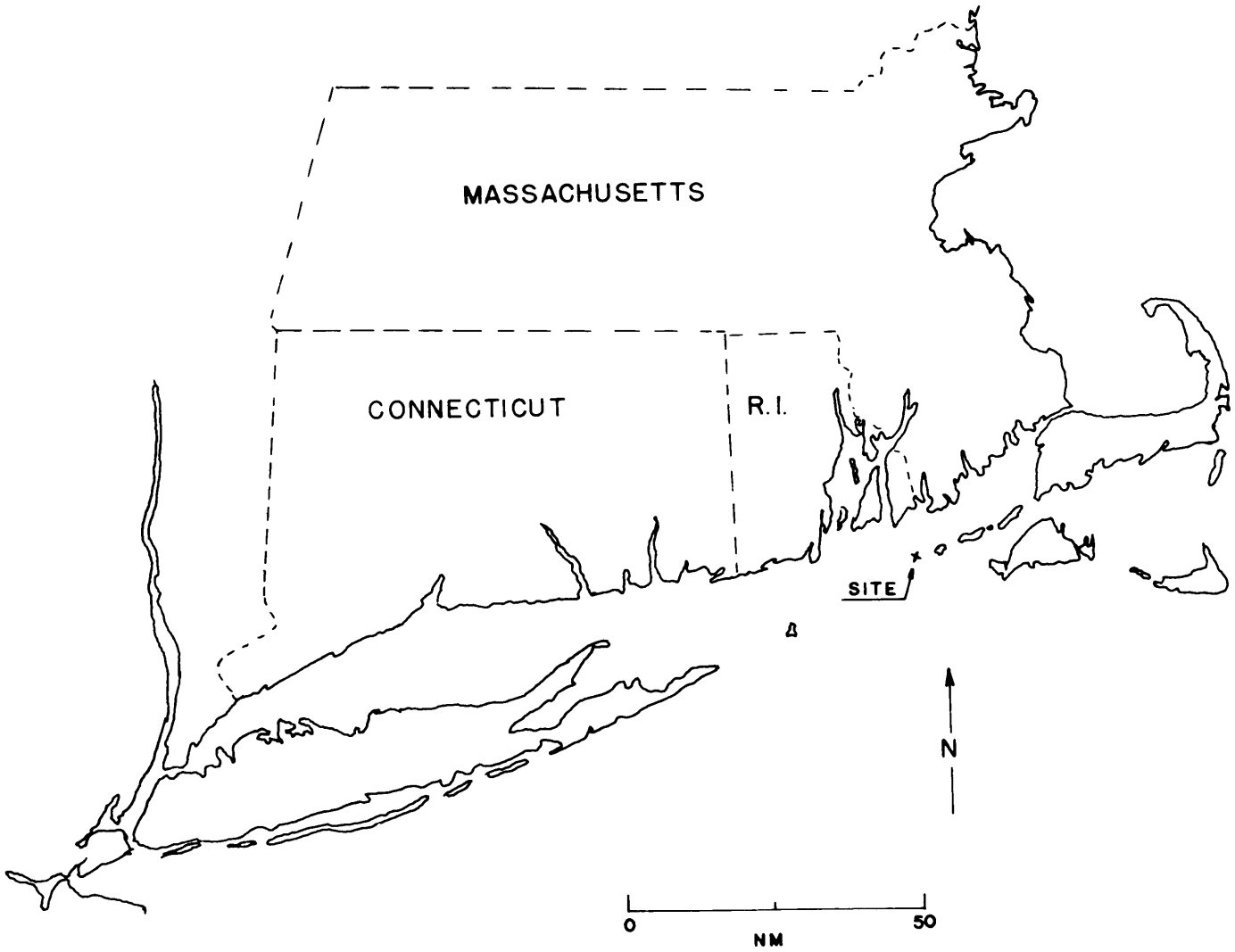

FIG. 1

for the work by Seesholtz (1968).

II.2 Spar

The instrument platform used in 1968 consisted of a 70 foot long radio transmission tower sitting on the bottom. This spar is shown in Figure 2. A five foot long spud on the lower end of the tower was jetted into the gravel bottom. The cross section of the tower was an equilateral triangle, a side being 2 feet long. Three smaller triangular struts served as lateral supports. These had a length of 60 feet each and led at an angle from the bottom to a point on the main tower 20 feet below the surface.

On the upper end of the tower a three by six foot platform, some ten feet above mean low water, provided the working area. The 20 foot mast, a three by six inch hollow rectangular steel beam, extended vertically above the platform. A pair of 12 foot long parallel booms, with an 8 foot vertical separation, were fastened to the tower with gooseneck joints and they supported at their outer end a 26 foot long pipe and the booms formed a parallelogram with the tower such that the instrument pipe remained vertical while the outer ends of the booms were raised or lowered with a topping lift. The pipe could also be rotated about its vertical axis. A board was fastened to the lower boom to allow access to some instruments when the rig was in its operating position.

Current magnitude was measured with a current meter fastened to the submerged lower end of the instrument pipe. A current vane was

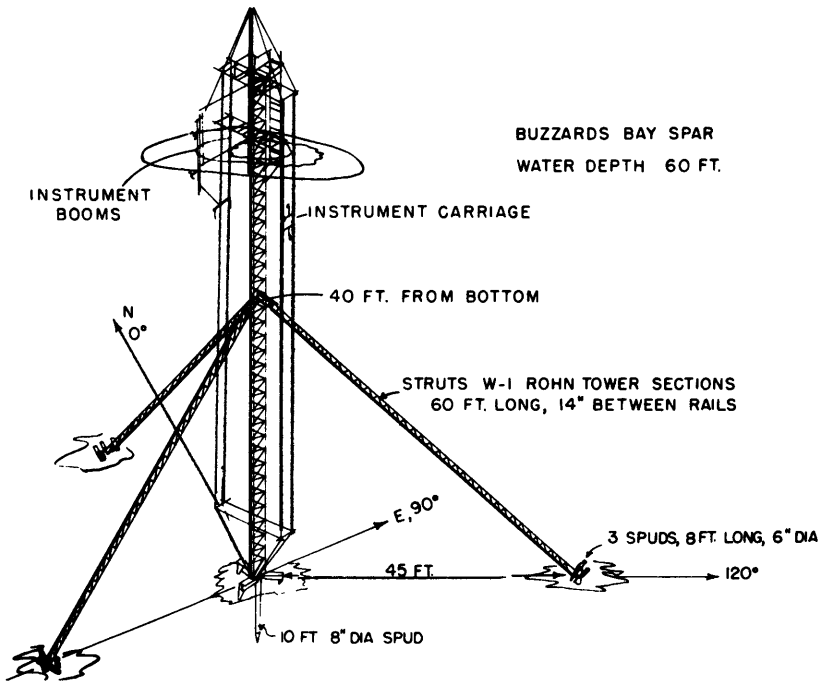
BUZZARDS BAY SPAR
WATER DEPTH 60 FT.
INSTRUMENT BOOMS
INSTRUMENT CARRIAGE
40 FT. FROM BOTTOM
N
0°
STRUTS W-I ROHN TOWER SECTIONS
60 FT. LONG, 14" BETWEEN RAILS
E, 90°
3 SPUDS, 8 FT. LONG, 6" DIA
45 FT.
120°
10 FT 8" DIA SPUD

Figure 2

bolted to the same end of the rotating pipe in order to always measure the current relative to the wave gauge array which was fastened to the same pipe and rotated with it. The current meter and vane were 2 meters below the surface in operating position. The support for the wave gauges was a horizontal aluminum frame in the shape of an H, clamped to the instrument pipe at its center and with its four ends guyed to the pipe. Wave gauges were fastened to all four ends of the H which formed a rectangle the sides of which were 3 and 5 meters. The array is shown in figure 3.

In addition to the Beckman and Whitley cup anemometer and wind vane on top of the mast (8.2 meters above mean low water), four Thornthwaite anemometers were fastened to the instrument pipe at points 1, 2, 3and 5 meters above the mean water level.

The height of the instruments relative to the water level was adjusted between data runs for tidal changes. Guys were used to swing the booms in azimuth in order to best bring the instruments to bear in the wind.

Motion of the spar was unnoticeable under operating conditions; under rough conditions the instrument pipe would undergo highly damped yawing oscillations when waves broke against it.

II.3 Boat.

The MIT research boat the R.R. Shrock moored for and aft about 100 feet downwind from the spar, supported instrumentation and data recording. A 175 foot umbilical signal cable, made up of 14 coaxial

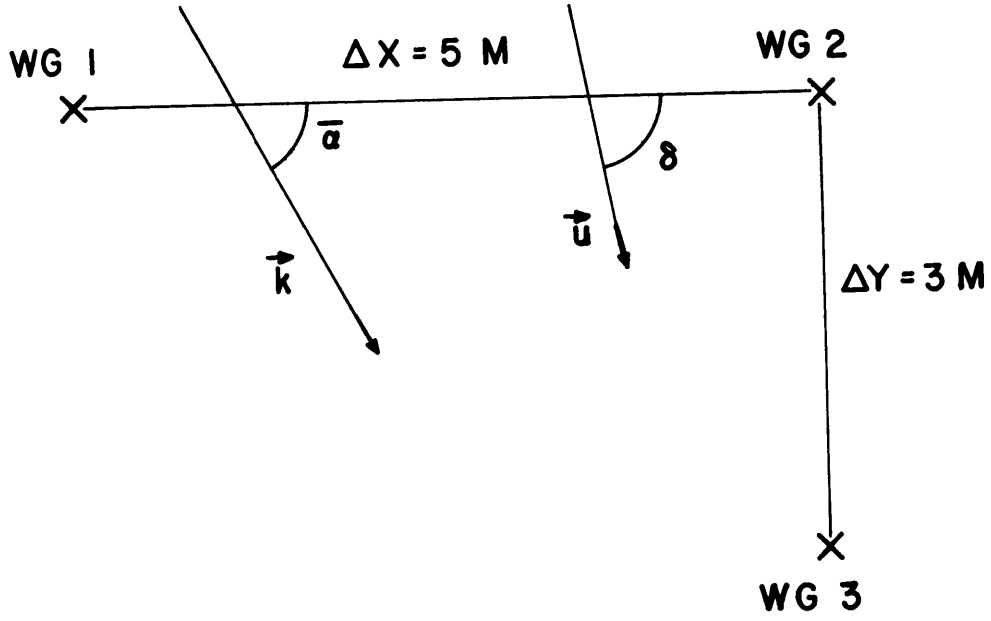

FIG. 3 WAVE GAUGE ARRAY

signal cables and two power cables with seven leads each, was strung in the water between the spar and the R.R. Shrock. The weight of the cables was taken up by styrofoam floats hooked to the umbilical at 15 foot intervals. On the spar the umbilical terminated in the "buoy box" to which all instruments were connected for their power and the regulated instrument power supplies. This generator was independent of the ship's own power system to prevent voltage fluctuations due to the ship's power needs.

II.4 Shore Facilities.

A decommissioned U.S. Coast Guard boat house on Cuttyhunk Island was obtained by MIT to serve as shore facilities of the project. The R.R. Shrock tied up to its pier every night or whenever no work was being done at the spar. Commuting from the dock on Cuttyhunk to the spar took about an hour each way.

The boat house contains a very large storage area and a workshop. A complete analog data analysis system, brought to Cuttyhunk for quicklook data analysis, was accommodated in the workshop along with all equipment necessary for servicing the instruments.

II.5 Instrumentation.

For transmission of the sensor output signals through the umbilical cable a frequency format was desired. All instruments built at MIT for this project were designed to have square wave signal outputs with frequency ranges between either 0 to 1 khz or 3 to 7 khz and a

peak to peak signal voltage of 15 volts. The advantage of the frequency format over analog signal outputs is self-evident to anyone who has attempted to transmit small voltage fluctuations over a long cable. Because all signal cables were coaxial no crosstalk problems were encountered.

Wave gauge

Wave height was measured using a capacitance type wave gauge designed and built by the Department of Meteorology at M.I.T.

The water level sensor is a 10 foot long insulated cable with a twisted multistrand wire core (outboard motor steering cable). The capacitance of the wire, which is proportional to water immersion, controls the frequency of an oscillator. This frequency was then mixed with a 30.1 khz standard frequency. The resulting output of the wave gauge was thus a square wave with a frequency variation between 300 and 700 hz for a change of 50 inches in waterheight. The relation between frequency and waterheight was linear. No temperature effects were noticed. The effect of dirt on the sensor was negligible except for oil; for this reason the sensor cables were periodically wiped clean with denatured alcohol. A frequency change for a 1 cm of water level change amounts to 2.88 hz and could be resolved.

In order to obtain the analog wave height it was necessary to demodulate the signals. This was done using modified demodulators which were part of the Beckman & Whitley wind system.

When taking wave data a 6 foot polypropelene line with a two pound sashweight on the end was hooked to the free end of the sensing cable

to keep it taut. The wave gauges performed free of trouble all summer and did not require any servicing aside from cleaning the cable.

Current meter

The current meter used as also designed and built at M.I.T. The principle of operation was a light beam interrupted by a chopping wheel connected to a propeller driven by the current. The light passed through light pipes to a photoresistor, which,with its associated circuitry, produced square output pulses. These were counted for two minute intervals. A vane kept the meter pointing into the current.

Current meter calibrations were run in the M.I.T. towing tank and gave a distance constant of 5.1 cm/count. The lowest speed obtainable in the tank was 30 cm/sec and no threshold was observed at this speed.

While the meter worked well under laboratory conditions it did not perform consistently in the field. It had to be serviced frequently. Since then a newer and better line of current meters has been built. A drogue was used as a current meter replacement. A small bucket, suspended three feet below the surface by a small surface float, was set adrift. Several drift times over a measured distance were obtained.

Beckman & Whitley Wind System

A Beckman & Whitley cup anemometer and wind vane was mounted at the masthead of the spar 8.2 meters above mean water. The system remained on the spar for the duration of the summer and was used to

measure mean wind conditions.

The frequency output of the six cup anemometer, compatible with the recording equipment, varied from 0 to 350 hz for wind speeds up to 30 mph. Frequency demodulators, which are part of the Beckman & Whitley wind system converted the frequency into analog signals. The output of the wind vane consisted of two 1 khz sine waves with a phase angle proportional to the wind direction. Part of the demodulating system translated this phase angle into a dc voltage. Wind direction was then plotted on a strip chart recorder aboard the R/V R.R. Shrock.

Thornthwaite Anemometers.

Four Thornthwaite anemometers were mounted on the instrument pipe at levels 1, 2, 3, and 5 meters above the surface. These four cup anemometers, manufactured by Thornthwaite Associates, are plastic and weigh seven grams total. Two-minute counts of pulses were obtained and printed out on Moduprints. The anemometers were calibrated by David Berrian and Kenneth Ruggles at the MIT low turbulence wind tunnel, a distance constant of 90cm was found.

II.6 Data Recording

A tape recorder, pulse counters with paper printout and strip chart recorders formed the core of the data recording equipment aboard the R/V R.R. Shrock

The model PI 6208 tape recorder, an eight channel recorder using 1/4 inch tape, manufactured by Precision Instruments of Palo Alto,

California, was used to record our data continuously for the length of the data run. Information can be recorded and played back at speeds of .375, 3.75 and 37.5 ips, inches per second, in either the direct or FM mode. FM signals of the correct frequency range (depending on the recording speed) when recorded in the direct mode are demodulated when played back in the FM mode. The recording speed chosen for this project was 3.75 ips and a maximum data run lasted ninety minutes, the time limit for 1800 feet of tape at that speed.

The wave gauge signals were recorded in the direct mode along with the Beckman & Whitley wind speed. The current direction was recorded periodically during a run. Wind direction was plotted directly on an Esterline-Angus strip chart recorder with a direct chart readout of wind direction in degrees true. In addition to being recorded the B & W wind speed and the current direction were counted on a pulse counter. Current magnitude (when working) and the four Thornthwaite pulses outputs were counted for two minute intervals and printed out.

Transmission through the umbilical cable caused some distortion to the square wave signals and it was necessary to reshape the signals prior to recording. An overdriven single transistor amplifier was used to reproduce a clean square wave without altering the frequency (and thereby the information) of the signal in any way.

On days considered to be suitable for data taking the R.R. Shrock was moored, the umbilical cable stretched to the spar, the cups

mounted and the rig placed in its operating position in a period of about three quarters of an hour (longer for rough days or new crew). Data runs lasted 45 minutes on the average since the rig had to be adjusted for changes in tidal height. Desirable data were thought to be those in which the sea was calm during rigging in the morning and then increased to 12 knots or more the middle of the afternoon.

III Theory

III.1 Theoretical basis of phase velocity measurements.

The ocean surface is quite successfully described as a large number of superpositions of solutions of the linearized equations which govern its motion. A single frequency component of the surface deformation is given as:

$$d\eta(\vec{x},t) = dA(\vec{k},\omega)\, e^{i(\vec{k}\cdot\vec{x}-\omega t)}$$

Here $\vec{x}$ is the position vector of an observation point relative to a reference frame, $\vec{k} = k\hat{k}$ with $h = |\vec{k}|$ is the wave vector and $\omega = 2\pi f$ the radial frequency. The above expression represents a wave, with an amplitude dependence on ω and k, propagating with phase speed $c_p = \frac{\omega}{k}$ in the direction of $\hat{k} = \frac{\vec{k}}{k}$. The dispersion relation obtained for this wave is $\omega^2 = (g\,k)\tanh(kh)$, g being the acceleration due to gravity and h the local water depth.

The total surface deformation, consisting of all wave numbers and frequencies, can then be given in terms of a Fourier-Stieltjes representation:

$$\eta(\vec{x},t) = \int_{-\infty}^{\infty} dA(\vec{k},\omega)\, e^{i(\vec{k}\cdot\vec{x}-\omega t)}$$

The cross-covariance of wave height observations $\eta_i(\vec{x},t)$ and $\eta_j(\vec{x}+\vec{r}_{ij},t)$ taken at points $\vec{x}$ and $\vec{x}+\vec{r}_{ij}$ respectively, is defined as:

$$R_{ij}(\vec{x},\vec{x}+\vec{r}_{ij},t,t+\tau) = \langle \eta_i(\vec{x},t)\,\eta_j(\vec{x}+\vec{r}_{ij},t+\tau)\rangle$$

τ is the amount of time the observation at point $\vec{x} + \vec{r}_{ij}$ is delayed with respect to the observation point $\vec{x}$.

In terms of the Fourier-Stieltjes representation the cross-covariance of the wave heights becomes

$$R_{ij}(\vec{x}, \vec{r}_{ij}, t, \tau) = \int_{-\infty}^{\infty}\int\int \Big[\langle dA_e(\vec{k}_e, \omega_e)\, dA_m(\vec{k}_m, \omega_m) \rangle\, e^{i(\vec{k}_e + \vec{k}_m)\cdot\vec{x}} \cdot e^{-i(\omega_e+\omega_m)t}\, e^{i(\vec{k}_m \cdot \vec{r}_{ij} - \omega_m \tau)} \Big] \qquad (3.1)$$

If the cross-covariance is independent of the origin and orientation of the reference frame but depends only on $\vec{r}_{ij}$, the separation vector of observation points i and j, the cross-covariance is homogenous. Similarly, if the cross-covariance depends on the delay time only and not on an absolute time scale, the wave field is considered to be stationary. With these conditions the average

$$\langle dA_e(\vec{k}_e, \omega_e)\, dA_m(\vec{k}_m, \omega_m) \rangle = \Psi(\vec{k}_m, \omega_m)\, \delta(\vec{k}_e + \vec{k}_m)\, \delta(\omega_e + \omega_m) \cdot d\vec{k}_e\, d\vec{k}_m\, d\omega_e\, d\omega_m$$

Where $\Psi(k,\omega)$ is the spectral wave energy density.

Substituting the last expression into equation 3.1 we obtain for the cross-covariance:

$$R_{ij}(\vec{r}_{ij}, \tau) = \int_{-\infty}^{\infty}\int \Psi(\vec{k}, \omega)\, e^{i(\vec{k}\cdot\vec{r}_{ij} - \omega\tau)}\, d\vec{k}\, d\omega \qquad (3.2)$$

The Fourier transform of the cross-covariance defines the co and quadrature spectra:

$$C_{ij}(\vec{r}_{ij},\omega)+iQ_{ij}(\vec{r}_{ij},\omega)=\frac{1}{2\pi}\int_{-\infty}^{\infty}R_{ij}(\vec{r}_{ij},\tau)\ e^{i\omega\tau}\,d\tau \tag{3.3}$$

The integration of the cross-covariance $R_{ij}\ (\vec{r}_{ij},\tau)$ can be performed in polar coordinates by defining $\xi = 0$ as an arbitrary direction of reference with which the observation point separation vector $\vec{r}_{ij}$ subtends the angle ρ_{ij} while the wave vector $\vec{k}$ subtends the angle ξ with the same reference line, as shown in Figure 4.

Then $d\vec{k} = k\,dk\,d\xi$ and equation 3.2 becomes:

$$R_{ij}(\vec{r}_{ij},\tau)=\int_{0}^{2\pi}\int_{0}^{\infty}\Psi(k,\omega,\xi)\ e^{ikr_{ij}\cos(\xi-\rho_{ij})}\ e^{-i\omega'\tau}\,k\,dk\,d\xi\,d\omega' \tag{3.4}$$

Equation 3.4 contains an integration over all wave numbers which are associated with the frequency ω. Under conditions for which linear potential wave theory is valid the theoretical linear dispersion relation shows that frequency is a single valued function of wave number, implying that:

$$\Psi(k,\omega,\xi)=\Phi(k,\xi)\,\delta(\omega-\omega') \tag{3.5}$$

where ω' satisfies the dispersion relation

$$\omega'^2=gk\tanh kh$$

It is understood that the above delta function contributes

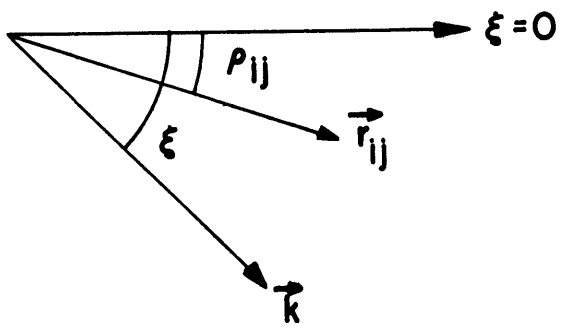

FIG.4 POLAR COORDINATES

only when ω and k satisfy the dispersion relation simultaneously. From now on it is assumed that wave number $k = k(\omega)$ is the wave number associated with the radial frequency ω.

Combining equations 3.5 and 3.4 with equation 3.3 yields the following integral for the cross-spectrum:

$$C_{ij}(\vec{r}_{ij},\omega) + iQ_{ij}(\vec{r}_{ij},\omega) = k\int_0^{2\pi} \Phi(k,\xi)\, e^{ikr_{ij}\cos(\xi-\beta_{ij})}\, d\xi \tag{3.6}$$

In general the form of the angular energy distribution contained in equation 3.6 is not known. If, for the time being, we assume only one direction of propagation, $\bar{\alpha}(\omega)$ for each frequency (A discussion of the form of $\Phi(k\xi)$ will be found in the section following this one.)

$$\Phi(k,\xi) = \varphi(k)\,\delta(\xi - \bar{\alpha}(\omega))$$

equation 3.6 can be integrated for this energy distribtuion and

$$C_{ij}(\vec{r}_{ij},\omega) + iQ_{ij}(\vec{r}_{ij},\omega) = k\,\varphi(k)\, e^{ikr_{ij}\cos(\bar{\alpha}-\beta_{ij})} \tag{3.7}$$

Since the cross-spectrum is complex quantity it can be written in polar form as:

$$C_{ij}(\vec{r}_{ij},\omega) + iQ_{ij}(\vec{r}_{ij},\omega) = |C_{ij} + iQ_{ij}|\, e^{i\Theta_{ij}}$$

with a phase angle:

$$\Theta_{ij} = kr_{ij}\cos(\bar{\alpha}-\beta_{ij})$$

Two cross-spectral phase angles are obtained by applying the expression for the cross-spectrum given by equation 3.7, to the wave gauge array shown in Figure 3 in which wave gauges 1 and 2 are separated a distance Δx along $\xi = 0$ (such that $\rho_{12} = 0$) and gauges 2 and 3 separated a distance Δy perpendicular to $\Delta x (\rho_{23} = \frac{\pi}{2})$:

$$\Theta_{12} = k \Delta x \cos \bar{\alpha}$$

$$\Theta_{23} = k \Delta y \sin \bar{\alpha}$$

This can be solved for k and the phase speed c_p:

$$k = \left[\left(\frac{\Theta_{12}}{\Delta x} \right)^2 + \left(\frac{\Theta_{23}}{\Delta y} \right)^2 \right]^{1/2} \tag{3.8}$$

and

$$c_p = \frac{\omega}{k} = \omega \left[\left(\frac{\Theta_{12}}{\Delta x} \right)^2 + \left(\frac{\Theta_{23}}{\Delta y} \right)^2 \right]^{-1/2}$$

The direction of propagation $\bar{\alpha}$ is

$$\bar{\alpha} = \arctan \frac{\Theta_{23}/\Delta y}{\Theta_{12}/\Delta x} \tag{3.9}$$

It is thus possible to calculate phase speeds, as function of frequency, from cross-spectral analysis of wave height measurements. While the phase speed analysis as just outlined is not restricted to any particular wave gauge array, it is very much

simplified when applied to the array chosen in this experiment. The cross-covariance of the third wave gauge pair in the array (formed from measurements by wave gauges 1 and 3) does not offer any new information and is therefore not used in the analysis.

Next we consider two wave fronts of the same frequency and energy content, propagating such that each wave vector subtends an angle β with the mean direction of propagation $\bar{\alpha}$ as shown below:

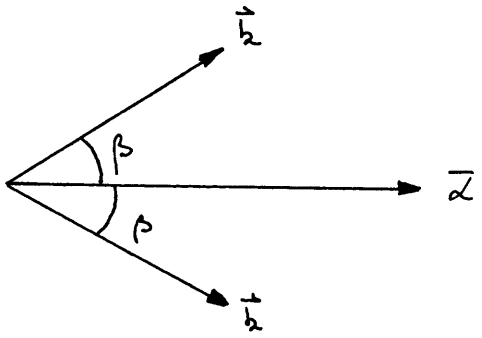

then

$$\bar{\Phi}(k,\xi) = \varphi(k)\left[\delta(\xi-(\bar{\alpha}+\beta)) + \delta(\xi-(\bar{\alpha}-\beta))\right] \tag{3.10}$$

For this energy distribution:

$$\Theta_{12} = k\Delta x \cos\bar{\alpha}\cos\beta \quad \text{and} \quad \Theta_{23} = k\Delta y \sin\bar{\alpha}\cos\beta$$

and

$$k_s = \left[\left(\frac{\Theta_{12}}{\Delta x}\right)^2 + \left(\frac{\Theta_{23}}{\Delta y}\right)^2\right]^{1/2} = k\cos\beta \tag{3.11}$$

The phase speed predicted for the total wave field is related to the phase speed c_p (the phase speed of each component) by

$$c_s = \frac{\omega}{k_s} = \frac{c_p}{\cos\beta} \tag{3.12}$$

Since $c_s \geq c_p$ the phase speed of the total wave field is larger than the phase speed of each component in the wave field. Phase speed measurements taken when wave spreading or multiple direction wave fronts exist should then exceed the phase speed measured for a single wave front.

III.2 The Angular Energy Distribution.

As was demonstrated in previous section, the exact form of the angular energy distribution $\Phi(k,\xi)$ has to be known in order to carry out the cross-spectral and phase speed analysis. The energy distribution for a general wave field is however not known theoretically and its measurement in the field is the object of directional spectral analysis (discussed in section III.3).

Theories of wave generation by wind advanced by Phillips (1957) and Miles (1957, 1959, 1960, 1962) suggest however a form of the angular distribution which is thought to exist when wave generation by wind takes place. The cross-spectral integrals and phase angles can then be evaluated for the suggested angular energy distribution and its resultant effect on phase speed can be compared to the phase speed predicted by the dispersion relation and eventually to actual phase speed measurements.

Phillips, in his resonant wave generation mechanism, predicts that waves, with phase velocity c_p, are generated at an angle (the resonance angle) to the wind eddy convection velocity U_c such that

$$\alpha = \arccos \frac{c_p}{u_c} \qquad (3.13)$$

and that the energy contained by these waves grows linearly with time.

For the convection velocity U_c Phillips (1965) assumes a value of 25 times the friction velocity u_* which is obtained from the logarithmic wind profile.

$$U(z) = \frac{u_*}{\kappa} \ln\left(\frac{z}{z_o}\right) \qquad (3.14)$$

where U(z) = wind velocity as a function of height z above sea level

u_* = friction velocity

κ = .42 = von Karman constant

z_o = roughness length

Lighthill (1962) suggests U_c to be value of the wind velocity at a height .2 wave length above mean sea level while Gilchrist (1966) chose the wind velocity at .25 wave length above the sea level for his value of U_c.

For a constant value of U_c the spread angle α of equation 3.13 increases with a decrease in phase speed and, since $U_c = 25\ u_*$ is usually larger than the wind speed at a height of .2 - .25 wave length above the surface, the spread angle predicted for a wave of a given frequency by Phillips is larger than the one predicted by either Lighthill or Gilchrist.

As the height of the resonantly generated waves increases it is believed that the resonance mechanism loses in importance and is replaced by Miles sheltering mechanism in which wave growth is exponential with time until non linear wave interaction predominate and an equilibrium spectrum is established. The frequency at which transition from the resonant mechanism to the sheltering mechanism occurs depends on the duration (or fetch) of the wind and can be estimated by Miles (1960) theory. For a given wind duration the same theory also shows that the Miles mechanism is approached sooner for waves propagating nearly parallel to the wind than for waves whose wave vectors subtend a large angle with the wind.

In view of these theories the angular distribution is assumed to be of the form:

$$\bar{\Phi}(k,\xi) = \frac{\varphi(k)}{2\sigma\sqrt{2\pi}}\left[e^{-\frac{(\xi-(\bar{\alpha}+\beta))^2}{2\sigma^2}} + e^{-\frac{(\xi-(\bar{\alpha}-\beta))^2}{2\sigma^2}}\right] \tag{3.15}$$

This bimodal distribution is symmetric about $\bar{\alpha}$, the mean direction of wave propagation. The gaussian lobes subtend an angle $\pm\beta$ with $\bar{\alpha}$ and the wave spreading of each lobe is proportional to the standard deviation σ . In the limit as $\beta \to 0$ the distribution reduces to an unimodal gaussian; as $\sigma \to 0$ it approaches two Delta functions, implying two very narrow beams of wave propagating with an angle 2β between them. As β and σ approach zero simultaneously, the distribution describes the wave propagating without any angular spread along $\bar{\alpha}$, as discussed in the previous section. The various distributions are shown in Figure 5 with $\bar{\alpha} = 0$.

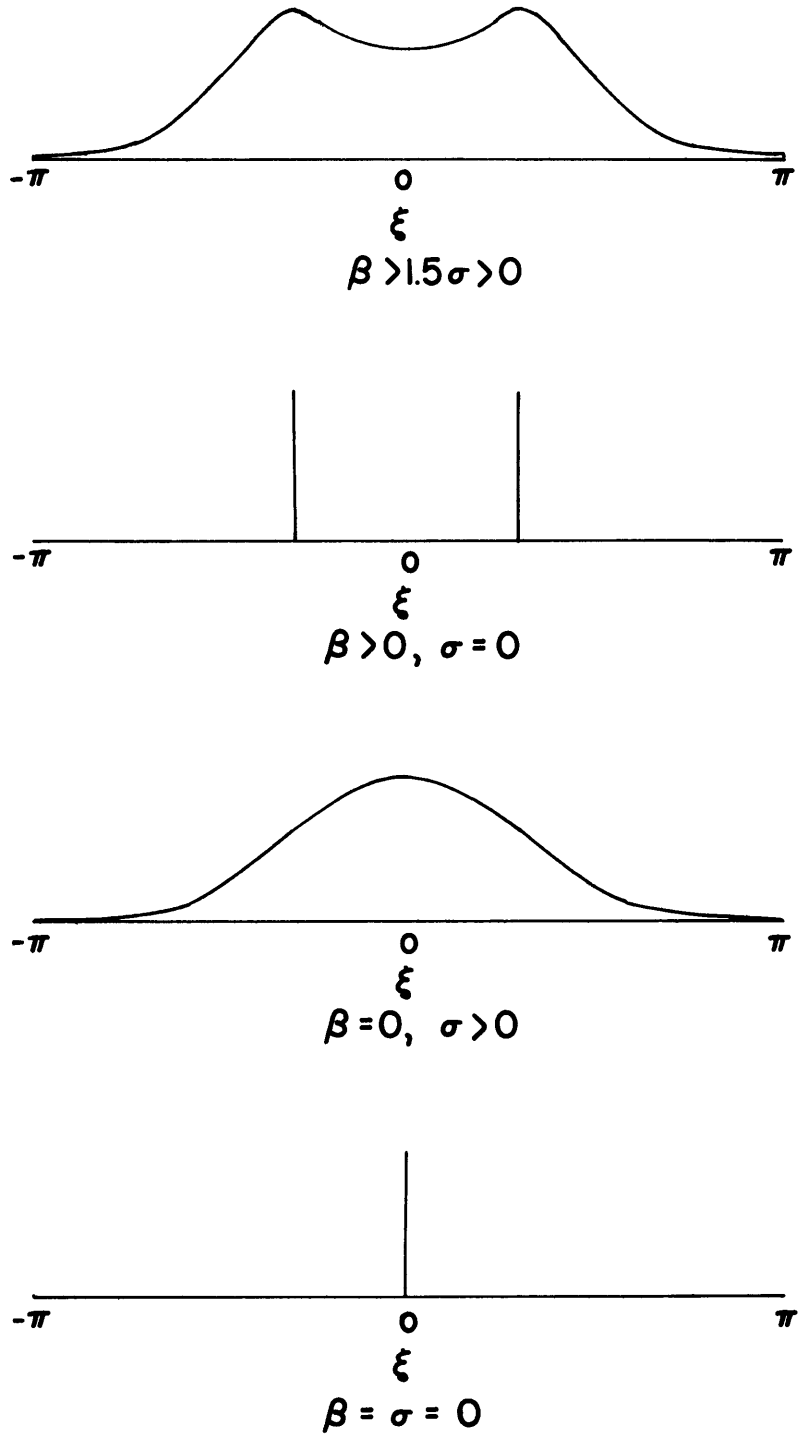

FIG. 5 PLOTS OF $\Phi(k,\xi)$ FOR VARIOUS VALUES OF β AND σ.

The reason for chosing this particular form for the angular distribution is as follows. Resonant wave growth is most effective at the resonance angles and waves of maximum energy are not found to propagate along the mean direction of propagation $\bar{\alpha}$ but rather at the resonance angles $\pm\alpha$ to the eddy convection velocity U_c, the direction of which is identified with $\bar{\alpha}$. When after sufficient wind duration or fetch, the resonance waves are of sufficient height, transition to Miles wave growth mechanism occurs. Waves of maximum energy, which propagate in the direction of the resonance angle, undergo transition first. Since transition of equally energetic waves occurs sooner for waves nearly parallel to the convection velocity than for waves which subtend a large angle with $\bar{\alpha}$, a gradual filling in of the center of the bimodal energy distribution should be expected to occur until the distribution is unimodal.

The cross-spectral analysis of equation 3.6 for the energy distribution suggested in equation 3.15 had to be carried out on a digital computer since no closed analytic solution to the integral 3.6 could be found. The results of the numerical integration follow.

$$\arctan \frac{\Theta_{23}/\Delta y}{\Theta_{12}/\Delta x} = \bar{\alpha}$$ = mean direction of propagation

and

$$k_s = \left[\left(\frac{\Theta_{12}}{\Delta x}\right)^2 + \left(\frac{\Theta_{23}}{\Delta y}\right)^2\right]^{1/2} \simeq k \cos\beta \cos\sigma \qquad (3.16)$$

The ranges of variables used in the integrations are shown in Table I.

The fact that the resultant wave number k_s (the "spread wave

RANGES OF VARIABLES USED IN THE CROSS-SPECTRAL INTEGRATION

FOR THE BIMODAL GAUSSIAN ENERGY DISTRIBUTION

k_{min}	k_{max}	Δk	α_{min}	α_{max}	$\Delta\alpha$	σ_{min}	σ_{max}	$\Delta\sigma$	β_{min}	β_{max}	$\Delta\beta$
.05 m^{-1}	.610 m^{-1}	.01 m^{-1}	1.5 rad.	1.5 rad.	--	.10 rad.	.70 rad.	.10 rad.	0 rad.	0 rad.	--
.1	.5	.1	1.5	1.5	--	.1	.1	--	0	1.0	.10
.4	.4	--	0	3.0	.30	.1	.1	--	.4	.4	--

Table I

number") is independent of $\bar{\alpha}$ is expected since the orientation of the array in the field should be immaterial. The relation between k_s and the true wave number k is to first order in β,σ and k:

$$k_s = k \cos\beta \cos\sigma \tag{3.17}$$

The above approximation compares well with the numerical results obtained for k_s for small values of $\sigma(\sigma < .35$ radians) with β varying between 0 and 1 radian. For larger values of σ the above relation deviates non-linearly in k, β and σ from the numerical values found for k_s. For a given value of k = .600 m^{-1} the value obtained by the above relation for k_s (equation 3.17) with $\beta = 0$, $\sigma = .70$ radian is .459 while the computed numerical result for k_s has a value of .490, a difference of 6.3%.

The phase speed of the total wave field, the angular distribution of which is given by equation 3.15 is given by

$$c_s = \frac{\omega}{k_s} = \frac{c_p}{\cos\beta\cos\sigma} \tag{3.18}$$

This result agrees in the limits as σ and or β go to zero with the results found in section III.1.

It is interesting to note that both σ and β enter into the expression for phase speed in the same order of importance. One cannot determine from actual phase speed measurements alone whether the angular distribution is as unimodal distribution ($\beta = 0, \sigma > 0$), a bimodal distribution ($\beta \neq 0$, $\sigma \neq 0$) or well defined wave fronts ($\beta > 0$, $\sigma = 0$).

The maxima of the bimodal energy distribution (given by equation 3.15) do not necessarily occur at the angles $\pm\beta$ but their position (given by μ) can be found from the equation

$$\beta' = \beta \tanh \frac{\beta'\beta}{\sigma^2} \qquad (3.19)$$

The three roots of the above equation are $\beta' = 0$ and $\beta' = \pm\mu$. If $\beta > \sigma$ the root $\beta' = 0$ corresponds to a relative minimum and maximum energy is found along the directions $\pm\mu$. It can further be shown that energy maxima occur at angles equal to or less than β and that $\mu \tilde{-} \beta$ for $\beta \gtrsim 1.5\sigma$. For the case $\beta < \sigma$ all three roots are zero and the energy maximum is found along the mean propagation direction $\overline{\alpha}$.

Since the energy maxima of the bimodal energy distribution are thought to be due to most active resonant wave generation, we identify the angles μ with the resonance angle given by Phillips we have from equation 3.13.

$$\cos\mu = \frac{c_p}{U_c} \qquad (3.13a)$$

and from equation 3.18

$$\cos\beta \cos\sigma = \frac{c_p}{c_s} \qquad (3.18a)$$

The principle values of β and σ can be found by solving equations 3.13a, 3.18a and 3.19 simultaneously using the observed values of c_s and U_c. It can however be shown that there exist specific solutions under the conditions listed below:

$U_c = c_s$	$\sigma = 0,\ \mu = \beta$
$U_c > c_s$	no solution

The case $U_c < c_s$ may or may not produce solutions for β and σ and the

equations need to be solved fully.

III.3 Directional Spectral Analysis

The method of choosing a form of the angular energy distribution $\phi(k,\xi)$ is contrary to the approach taken in directional spectral analysis which determines the angular distribution from cross-spectral measurement.

By expanding the distribution $\phi(k,\xi)$ in the series

$$\Phi(k,\xi) = \sum_{n=0}^{\infty} A_n \cos n\xi + B_n(k) \sin n\xi \qquad (3.20)$$

and substituting the expansion into the general cross-spectral integral given by equation 3.6, Barber (1963) has obtained a series expansion for the co and quadrature spectrum:

$$C_{ij}(\vec{r}_{ij},\omega) + iQ_{ij}(\vec{r}_{ij},\omega) = k \sum_{n=0}^{\infty} i^n \left[A_n(k)\cos n\beta_{ij} + B_n(k)\sin n\beta_{ij}\right] J_n(kr_{ij}) \qquad (3.21)$$

where $J_n(kr_{ij})$ is the Bessel function of order n.

By applying equation 3.20 to each wave gauge pair ij in the array a set of linear algebraic equations is generated. On the left hand side of each equation is the determined value of the co and quadrature spectrum while the right hand side contains the series expansion given by equation 3.21 for the wave gauge pair under consideration. These equations are then split into their real and imaginary parts. For an array with n wave gauge pairs, which yields n independent cross-spectra, there exist then 2n + 1 equations (the extra equation is due to an auto spectrum). A set of 2n + 1 linear algebraic equations can only be solved for 2n + 1 unknown coefficients A_n & B_n. Since arrays usually consist of a finite (and small) number of wave gauges,

it is necessary to truncate the series expansions, given by equation 3.20 and 3.21, with the hope that higher order coefficients are negligible. The calculated energy distributions then give approximations to the true energy distribution. The quality of the approximation depends on both the number of wave gauges and their geometric arrangement in the array.

Since the truncated series contains coefficients of low order in n(and has trigonometric function of low multiplies of angle ξ) only, it is not surprising that the directional resolution is low and the calculated energy distribution of a single theoretical wave front (with a true distribution $\Phi(k,\xi) = k\phi(k)\delta(\xi-(\bar{\alpha}-\beta))$ shows considerable spread and uncertainty of direction of propagation.

The quality of the approximate energy distribution was tested for the wave gauge array used in this study by assuming a true energy density $\Phi(k,\xi) = k\phi(k)[\delta(\xi-(\bar{\alpha}+\beta)) + \delta(\xi-(\bar{\alpha}-\beta))]$ and calculating the cross-spectra appropriate for the wave gauge array shown in Figure 3. A set of equations was generated and solved numerically for the coefficients A_n and B_n. The approximate energy distribution for various values of $\bar{\alpha}$ and with $\beta = 0$ is best described as a distorted, asymetric curve slightly resembling a gaussian having a deviation of roughly $\pm \pi/8$ centered on or near the angle $\bar{\alpha}$. For the bimodal distribution ($\beta \neq 0$) the distribution is even less recognizeable since it is dominated by a single large cosine function. Some of the directional spectra calculated for theoretical directional spectra given by Delta functions are shown in Figure 6.

While it may appear that a Delta function wave vector is a very stringent test it should be pointed out that the directional resolution

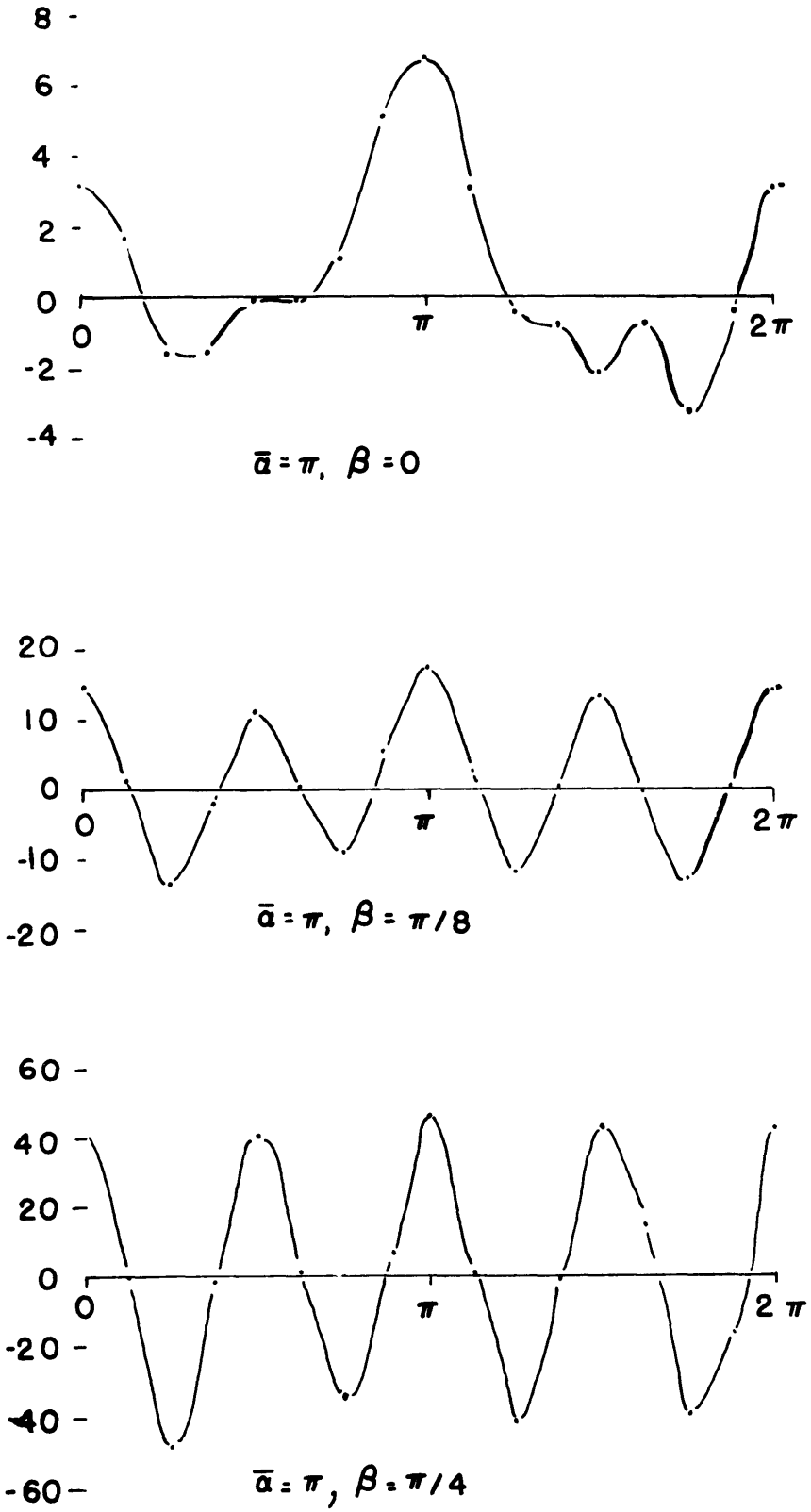

FIG. 6 COMPUTED THEORETICAL DIRECTIONAL SPECTRA

must be very high in order to distinguish between a wide unimodal or a narrower bimodal distribution. It is the author's contention that the directional spectral analysis has too low a resolution to clearly differentiate between an unimodal or bimodal angular energy distribution and is thus of no value in this study.

III.4 Current Effects on phase velocity

A steady current bodily advects waves. Wave frequencies and velocities measured in a frame at rest relative to the bottom will differ from those measured in a frame moving with the current $\vec{u}$. This was pointed out in a paper by Whitham (1960). The relation between the velocities is given by: $\vec{c}_m = \vec{c}_p + \vec{u}\cdot\hat{k}\,\hat{k}$

where $\vec{c}_m$ is measured in the frame at rest and in the presence of $\vec{u}$. This relation relies on the fact that a Galileian transformation between the two reference frames leaves the wave vector $\vec{k}$ unchanged. In terms of the angles defined in Figure 3 the expression for the corrected phase speed for a single wave vector is

$$|\vec{c}_p| = |\vec{c}_m| - |\vec{u}|\cos(\bar{\alpha} - \delta) \tag{3.22}$$

where $\bar{\alpha}$ has previously been defined. A similar correction for frequency is given by

$$\omega = \omega_m - |\vec{u}|k\cos(\bar{\alpha} - \delta) \tag{3.23}$$

Current effects are more important for waves with a low phase speed and the frequency correction becomes larger for larger wave numbers.

IV. Data Analysis

IV.1 Analog Data Analysis

Originally all data analysis was to be performed using analog techniques. Since the frequency of the wave information in this study is centered about .25 hz it was necessary to speed up the data by a thousand in order to be able to use available analog analysis equipment. The data speed up was accomplished by re-recording the data, already speeded up ten times, on a second tape recorder equipped with a tape loop attachment. This tape loop was then played back at a speed 100 times faster than it was recorded. A twenty minute "real" time record was thus compressed into a record with a period of 1.2 seconds which was continuously played over and over into the data analysis system. An extensive description of the analog data analysis system is given by Seesholtz (1968).

One of the main drawbacks encountered in analog processing was that the bandwidths of the available filters were too wide with respect to the spectra, causing a large amount of spectral smoothing of the results when trying to analyze a small frequency interval. A further problem was presented by the tape splice of the loop. Depending on the quality of the splice, which did not always seem to be proportional to the amount of care taken in splicing, harmonics of the splice could appear over the whole spectrum. The third disadvantage of our system was its inability to perform higher order statistics such as cross-spectra.

It was then decided to process the data on a digital computer.

The data were digitized and a program containing several specialized subroutines for this particular study was written.

IV. 2 Digitization of Data

The data points for the computations were obtained by digitizing the analog record on the analog-digital computer system of the Department of Mechanical Engineering at M.I.T. A maximum of 16 channels of information can be sampled by the analog computer up to 6000 times per second with a skew of 100 microseconds between samples. The 20 volt input range is divided into 1023 sampling intervals with an accuracy of ± 1 in the last place. The digital voltmeter output is transferred from the analog computer to the IBM 1130 computer which stores and also sorts all data points by channel. The output of the system are punched cards with 56 bipolar binary data points per card.

In order to get the data in a form compatible with the digitizer, recorded tapes containing the demodulated and amplified wave data were prepared. A calibration signal was recorded on the beginning of each tape for each channel containing wave gauge data. This signal was obtained by the demodulation and amplification, in precisely the same manner as the wave information, of a constant frequency corresponding to a change in water level of 20 cm. This calibration signal was chopped into square waves by a relay prior to being recorded.

Before digitizing the data signal levels were preamplified so to utilize the ± 10 volt input range as much as possible in order to

reduce quantization errors. DC voltage levels in the record were removed by an adjustable bias control on the preamplifiers. To insure against any data loss by saturating the preamplifiers the entire records were traced on a storage oscilloscope.

To reduce computer time digitization was done at a data speed up of 10. A 200 millisecond ("real" time) time interval was chosen and roughly 10^4 points per channel were taken. For a record of 8 channels with 10^4 points each about 40 minutes of computer time is required, most the time being taken up by the card punch.

IV.3 Computation

The actual computations were carried out on the IBM 360/65 of the Computation Center at M.I.T. To a large extent the program was written by Kenneth Ruggles at M.I.T. according to standard statistical methods as described, for example, by Bendat and Piersall (1966). This program was designed to handle up to four data channels of 9600 points at one time.

After the means and linear trends were calculated and removed for each channel variance, skew and kurtosis were computed. Up to 10 auto or cross-covariances and the same number of auto or cross-spectra can be evaluated, printed out, punched on cards or plotted on a Calcomp plotter as desired. Specialized subroutines performed additional computations and will be described in the following paragraphs.

Calibration

Before any computations were carried out the first 1500 points of each wave gauge channel were printed out. This was done to obtain the calibration signal and to find out where the calibration signal ended and the data began. Since the calibration signal was a square wave, the difference between the maximum and minimum value corresponds to a water level difference of 20 cm. From this a multiplier was found for each wave gauge. On subsequent computations all input data were multiplied by the appropriate constant. The results were then calibrated in cm (cm^2 sec for waves energy spectra.)

Digitizing Interval

As stated previously, the data were digitized at 200 millisecond intervals corresponding to a Nyquist frequency of 2.5 hz, much above our frequency range of interest. An option incorporated in the program made it possible to use, for computations only, every other data point, thus doubling the time interval (Δt) to 400 msec with a folding frequency of 1.25 hz, still 5 times higher than the significant peak in our spectra. While there is an obvious reduction in computation time obtained by cutting the data points and number of delay lags in half, the spectral resolution and error of spectral estimates remain the same.

Cross-Covariance

Cross-covariances between records x and y were computed using the following equations:

$$R_{xy}(r[\Delta t]) = \frac{1}{N-r}\sum_{n=1}^{N-r} x_n\, y_{n+r}$$

$$R_{yx}(r[\Delta t]) = \frac{1}{N-r}\sum_{n=1}^{N-r} x_{n+r}\, y_n$$

The index r denotes the number of the lag and goes from 0 to m; delay time τ equals the lag number times the digitization interval. For zero delay time the value of the auto-covariance (when x = y) is equal to the variance of the record since the mean of each record was set to zero; the auto-covariance is also an even function of the delay time.

Cross-Spectra

Cross-spectra are simply the Fourier transform of cross-covariances and were computed using the formulas given by Bendat and Piersall (1966). The expressions for the unsmoothed co-spectra are:

$$C_{xy}(\omega) = 2(\Delta t)\left[A_0 + 2\sum_{r=1}^{m-1} A_r \cos(\omega r \Delta t) + A_m \cos(\omega m \Delta t)\right]$$

while the raw quadrature spectra are given by:

$$Q_{xy}(\omega) = 2(\Delta t)\left[2\sum_{r=1}^{m-1} B_r \sin(\omega r \Delta t) + B_m \sin(\omega m \Delta t)\right]$$

where

$$A_r = \frac{1}{2}\left[R_{xy}(r\Delta t) + R_{yx}(r\Delta t)\right]$$

and

$$B_r = \frac{1}{2}\left[R_{xy}(r\Delta t) - R_{yx}(r\Delta t)\right]$$

For auto-spectra the value of B_r are zero for all lags r and their quadrature spectra are zero.

The frequencies $f = \frac{\omega}{2\pi}$ at which the spectra are computed are given in terms of the harmonic number ℓ :

$$f = \frac{\ell}{2m(\Delta t)} \quad , \quad \ell = 0, 1, 2 \ldots . \; m$$

When analyzing a record of finite length undersireable "window" effects are noticed which are corrected by smoothing or "Hanning" the raw spectral estimates. In this process the interior spectral estimates are smoothed in this manner:

$$C_\ell = \tfrac{1}{4} D_{\ell-1} + \tfrac{1}{2} D_\ell + \tfrac{1}{4} D_{\ell+1} \quad , \quad \ell = 1, 2 \ldots \; m-1$$

For the end points:

$$C_0 = \tfrac{1}{2} D_0 + \tfrac{1}{2} D_1$$

$$C_m = \tfrac{1}{2} D_{m-1} + \tfrac{1}{2} D_m$$

Here D denotes both the co and quadrature components. The phase angles are now very easily computed from the co and quadrature spectral estimates:

$$\Theta_{xy}(\omega) = \arctan \frac{Q_{xy}(\omega)}{C_{xy}(\omega)}$$

The spectral resolution Δf of the spectra equals

$$\Delta f = \frac{1}{2m(\Delta t)}$$

It should be noted that an increase in the time interval decreases the resolution. For a given resolution we can then increase Δt (with proper regard to the Nyquist frequency) while we decrease the total number of lags.

For waves, which are considered random in nature, the energy spectra are assumed to have error distributions of the Chi-square type. The numbers of degrees of freedom, n, depends on the total number of data points N and the maximum number of lags, m, in the cross-covariance:

$$n = \frac{2N}{m}$$

If the number of degrees of freedom is larger than 30, the χ^2 distribution approaches a Gaussian distribution and the unit standard error is given by:

$$\varepsilon = \sqrt{\frac{m}{N}}$$

There exists then a choice between the frequency resolution and the error that is acceptable. Since the effective bandwidth is inverse to the number of lags used to compute the cross-covariance, but the error is proportional to the square root of the same number, a trade off between the two is needed. We then can construct the table of $\Delta f/\varepsilon$ shown below:

	N = 4800		N = 9600
	Δt = .2 sec	Δt = .4 sec	Δt = .2 sec
m = 50	.05 / .104	.025 / .104	.05 / .071
m = 100	.025 / .42	.0125 / .142	.025 / .104
m = 200	.0125 / .204	.006125 / .204	.0125 / .142

Since a resolution bandwidth of $\Delta f = .0125$ hz proved to be sufficient to differentiate between the spectral peaks of the swell and the wind driven sea, 4800 data points, with a time interval of .4 sec and 100 lags were chosen for the cross-spectral computations.

Coherence

An important measure of the quality of cross-spectral analysis of records from two separated wave gauges is found in their coherence. The coherence is defined as

$$\gamma_{ij}(\omega) = \frac{|C_{ij}(\omega) + iQ_{ij}(\omega)|}{\sqrt{C_{ii}^2 + C_{jj}^2}}$$

The value of $\gamma_{ij}(\omega)$ ranges from 0 to 1, 0 implying no coherence whatsoever while a value of 1 denotes perfect agreement between the two records.

One important use of coherence is the determination of the statistical errors in cross-spectral phase angle analysis. This expression for the error was found by Goodman (1957) to be:

$$\sin^2 \Delta\Theta = \left[(1-P)^{-\frac{2}{n}} - 1\right] \frac{1 - coh_*}{coh_*} \tag{4.1}$$

The error is $\pm\Delta\theta$, P the confidence value, n the number of degrees of freedom and coh* is the true coherence which is assumed

to equal the measured coherence γ. P is then the probability that, for a given coherence and with n degrees of freedom, the true phase angle falls within $\pm \Delta\theta$ radians of the computed value.

Measured Phase Speed

The measured speed c_m of gravity waves in the open ocean was obtained using statistical data analysis on wave height measurements taken simultaneously by three wave gauges arranged in a triangular array, which is described in section II.5 and shown schematically in Figure 3.

Three wave gauges, numbered 1, 2, and 3 contained a right angle. The separation Δx between gauges 1 and 2 is 5 meters, the distance Δy, between wave guages 2 and 3 is three meters. Angle $\bar{\alpha}$, which is a function of frequency, is the angle contained by the wave vector and the wave gauge pair 12 as shown. The current vector makes an angle δ with the same wave gauge pair. The magnitudes of the measured phase speeds were calculated as functions of frequency by the expression:

$$C_m(\omega) = \omega \left[\left(\frac{\theta_{12}}{\Delta x} \right)^2 + \left(\frac{\theta_{23}}{\Delta y} \right)^2 \right]^{-1/2} \tag{4.2}$$

where the subscripts refer to the wave gauge pair under consideration. The mean propagation direction $\bar{\alpha}(\omega)$, as defined in Figure 3, was found from:

$$\bar{\alpha} = \arctan \frac{5.00}{3.00} \frac{\Theta_{23}(\omega)}{\Theta_{12}(\omega)}$$

(4.3)

The statistical errors in phase speed measurements depend on the phase angle error $\Delta\theta$ as defined previously. Upper and lower limits of measured phase speed errors (denoted by c_{mu} and c_{ml} respectively) were calculated by the expression:

$$c_m \begin{Bmatrix} l \\ u \end{Bmatrix} = \omega \left[\frac{(\Theta_{12} + \Delta\Theta_{12})^2}{(5.00)^2} + \frac{(\Theta_{23} + \Delta\Theta_{23})^2}{(3.00)^2} \right]^{-1/2} \quad \left[m/sec \right]$$

(4.4)

This means that the phase speed, c_m, will fall between c_{mu} and c_{ml} with the probability P for which the values $\Delta\theta_{12}$ and $\Delta\theta_{23}$ were computed. The measured coherences of wave gauge pairs 12 and 23 must used to calculate the respective errors $\Delta\theta_{12}$ and $\Delta\theta_{23}$.

At this point it may be helpful to recapitulate the various phase speeds encountered in this study:

1. c_p is the phase speed predicted by the dispersion relation $\omega^2 = g\ k \tanh(kh)$ such that $c_p = \omega/k$.
2. c_s is the phase speed which should be observed because of the assumed energy spreading $\Phi(k,\xi)$ as discussed in section III.2. Each individual wave propagates at phase c_p while $c_s = w/k_s$ and $k_s \leq k$.

3. c_m is the phase velocity calculated from actual wave height measurements according to the procedure in section IV.3. Here $c_m = \omega/k_m$.

V. Results

Of the data collected for phase speed measurements during the summer of 1968 four records were chosen for digital analysis. Two of these records were however found to lack sufficient wind information to warrant further analysis. The two remaining records which were analyzed in detail were both obtained on the 9th of August 1968. Each record contains thirty-two minutes of wave height information, the record marked AM was taken from 1159 am to 1231 pm while the record marked PM was obtained between 1435 and 1507.

Phase speeds (c_m) were calculated for these wave data using the methods described in section IV and compared to the theoretical phase speed (c_p) given by linear dispersion relation for gravity waves. An increase of the measured phase speed c_m over c_p is considered to be due to wave spreading. This measured wave speed is then compared to the angular energy distribution suggested by equation 3.15 and the spread predicted by Phillips' resonance wave generation theory.

V.1 Wind and Current conditions

The wind and current conditions encountered during the AM and PM data runs are summarized in Table II.

The wind data of 9 August AM and PM were investigated by Ruggles (1969) who found a correlation coefficient of 1.00 between the observed and the logarithmic wind profiles.

Table II

Conditions for 9 August 1968

	AM	PM
1m anemometer	3.42 $\pm$ .50 m/sec	5.45 $\pm$ .38 m/sec
2m anemometer	3.55 $\pm$ .95 m/sec	5.96 $\pm$ .40 m/sec
5m anemometer	4.18 $\pm$ .63 m/sec	6.55 $\pm$ .38 m/sec
10manemometer	4.68 m/sec	7.20 m/sec
wind direction	232°-220°-232° True	236 $\pm$ 2° True
Fetch	> 26nm	> 26nm
current mag (u)	(.15$\pm$.075 m/sec)	.15 $\pm$ .075 m/sec
current dir (δ)	1.83 $\pm$ .1 rad	.524 $\pm$ .05 rad
u_*/κ	.4815 m/sec	.6897 m/sec
z_o	.00733m	.000304 m

Note: The current magnitude for the AM record was estimated to be the same as for the PM record.

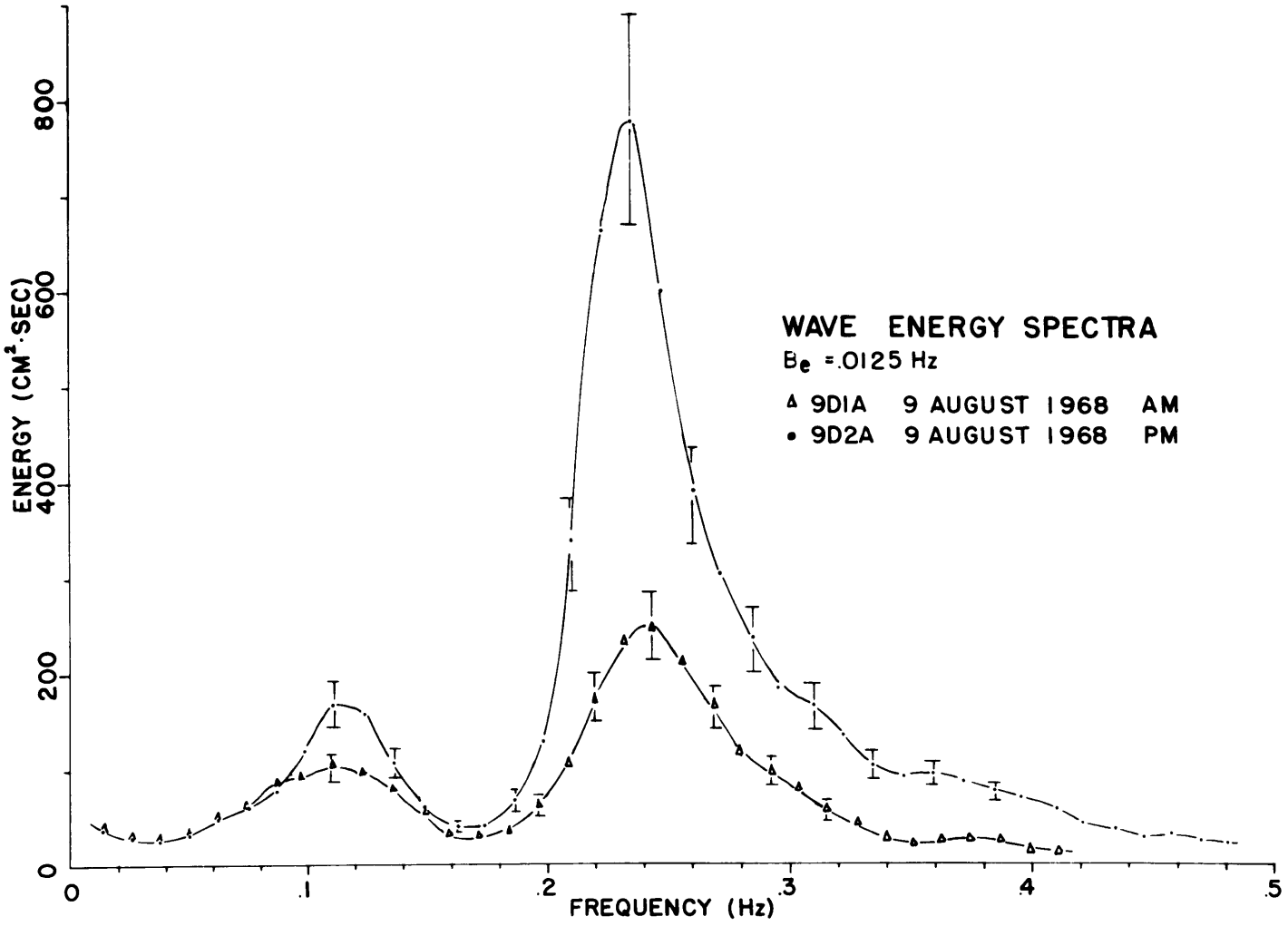

FIG. 7 WAVE ENERGY SPECTRA

V.2 Energy Spectra

The wave energy (auto) spectra for the two records are shown in Figure 7. Based on 4800 points with a time interval of .4 seconds and 100 correlation lags the number of degrees of freedom is 96, resulting in error bars very close to the standard deviation of .142 which are shown. The frequencies of the spectra have been corrected for advection by iterating the dispersion relation:

For an initial wave number k the frequency ω was found from the dispersion relation:

$$\omega^2 = gk \tanh kh$$

for a water depth of h = 19 meters. Next the current advection, given by equation 3.23, is applied to ω to yield ω_o such that

$$\omega_o = \omega + uk \cos(\bar{\alpha} - \delta)$$

where δ(the direction of the current with respect to the wave gauge array) is obtained from the current direction meter and $\bar{\alpha}$ is found from the measured phase angles as defined by equation

3.9. The frequency ω_o is then compared to a frequency ω_m for which cross-spectral analysis was performed. If $\omega_o = /\omega_m$ the value of the initial k was replaced by $k + \Delta k$ and the procedure repeated until $\omega_m = \omega_o$ with an error of less than one in thousand.

The value ω which yielded the advected value ω_m is then the corrected frequency while the final wave number k is the theoretical wave number associated with ω. This method used for the frequency correction made no use of the measured wave number k_m.

The modulus, $(C^2 + Q^2)^{1/2}$, and phase angle θ are plotted in Figure 8 for the corss-spectrum of wave gauge pair 23 of 9 August PM. The cross-spectral energy spectrum for both wave qauge pairs is very similar to the auto spectrum of any of the wave gauges. Since the wave gauge pair 23 is roughly parallel to the mean direction of propagation of the wave field phase angle θ_{23} increases more rapidly with frequency than the phase angle θ_{12} which is formed by the wave gauge pair roughly parallel to the wave crests.

V.3 Coherence

The coherence functions γ(as defined on page 47) are shown in Figure 9 for the wave gauge pairs 12 (denoted by γ_{12}) and 23 (denoted by γ_{23}). These curves are essentially concave downward with the coherence maxima at the spectral peaks of the swell and wind

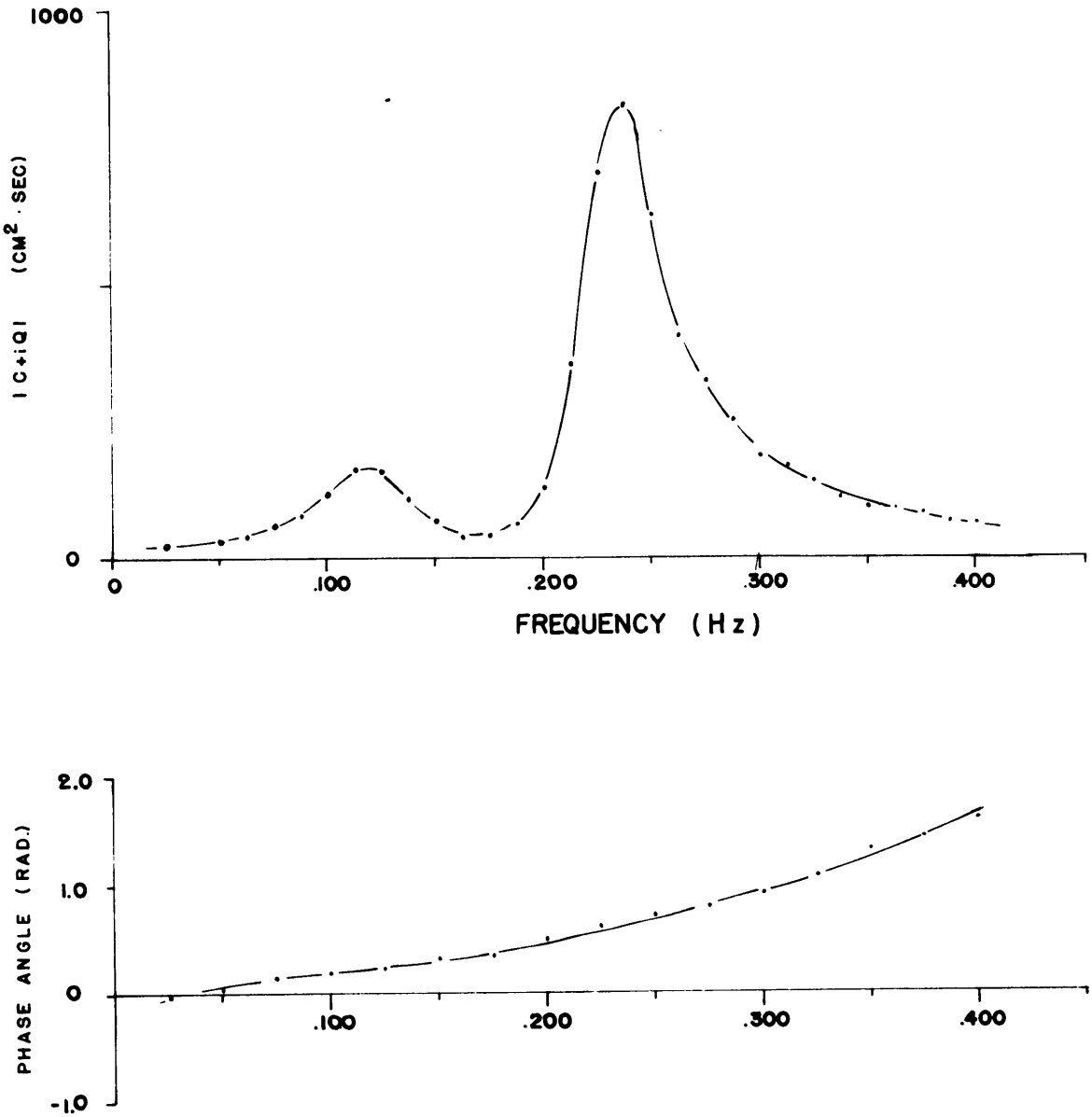

FIG. 8 CROSS-SPECTRUM OF WAVE GAUGE PAIR 2·3 OF 9 AUG. PM

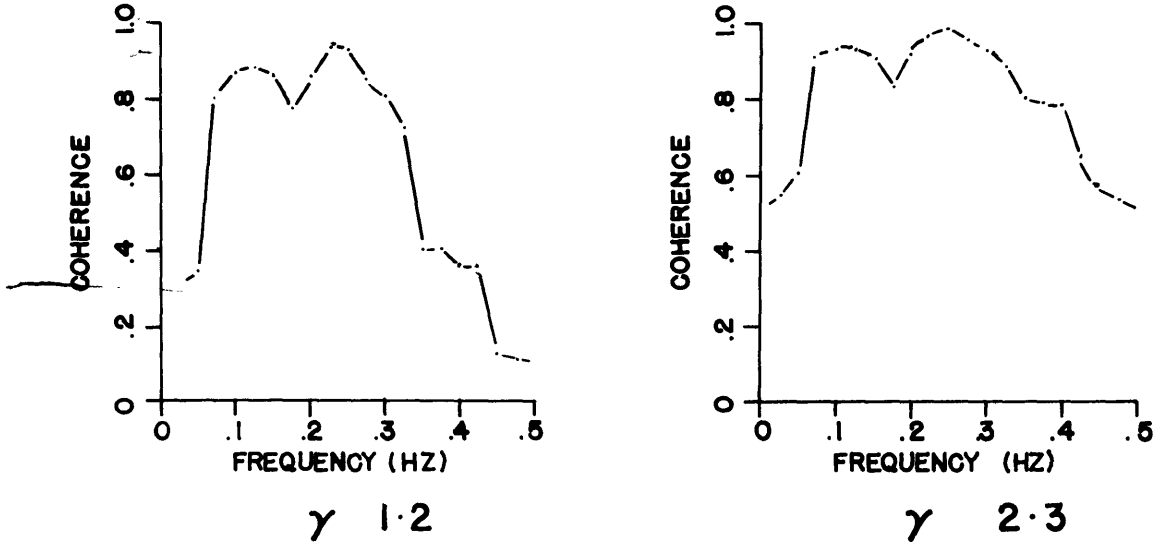

9 AUGUST AM

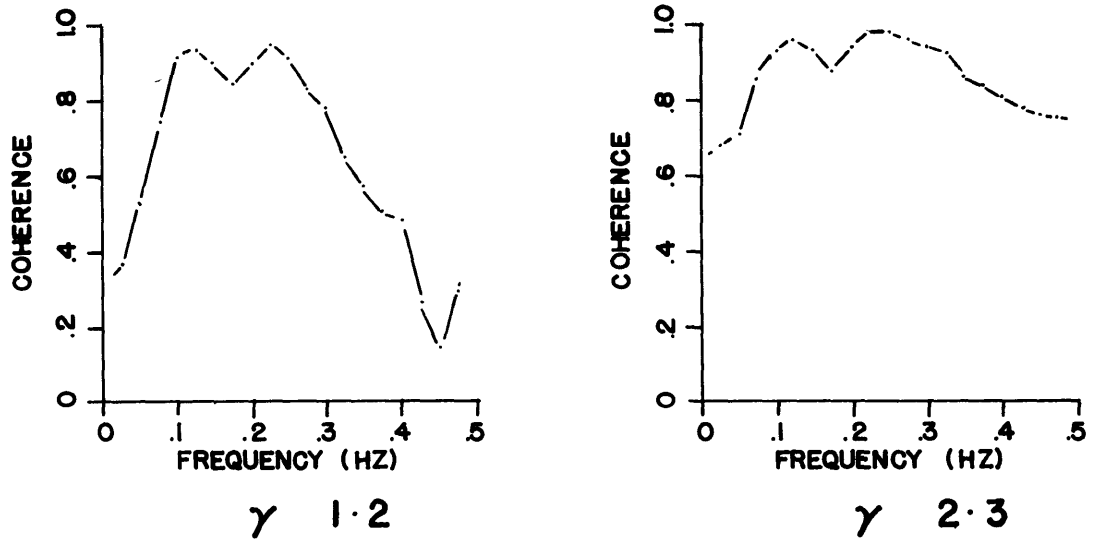

9 AUGUST PM

FIG. 9 COHERENCE SPECTRA

sea separated by relative minima occuring at the same frequency as the energy minima.

At frequencies above the wind sea the decrease in coherence is due to two effects: One is the shortness of wave crests for higher frequency waves, this is borne out by the fact that the coherence is higher for the wave gauge pair (in this case 23) which is oriented along the direction of propagation than for the pair (12) nearly parallel to the crests.

The second effect on the decrease of observed coherence values is the existence of several wave fronts of the same frequency. This effect has been shown theoretically by Munk, Miller, Snodgrass and Barber (1963). In the same paper it is stated that the use of coherence measurements as means to obtain directional spectra is "hazardeous at best."

The orientation of the mean propagation angle $\overline{\alpha}$ with respect to the wave gauge array has a predominant effect on coherence values calculated for the bimodal energy distribution; no coherent results could be found on comparing the predicted with the measured coherence. Coherence measurements have thus little value in establishing the angular energy distribution.

V.4 Phase Speed Measurements

The measured phase speeds c_m are calculated from cross-spectral phase angles as functions of frequency according to equation 4.2. Figures 10 and 11 show these speeds for 9 August AM and PM together

with error bars computed for 65% confidence interval using equation 4.4. Instead of applying the current correction to the measured phase speeds we assign error bars, which depend on the current, to the theoretical phase speeds shown as solid curves in Figures 10 and 11. Theoretical phase speeds, for different water depths but without current effects, are shown in Figure 12.

The frequency range for which the phase speed measurements are considered acceptable is not well defined. For spatial cross-covaraiances it is necessary (Kinsman (1965)) that the wave gauges are separated no more than 1/2 of the shortest wave length to be investigated. During data runs on 9 August the wave gauge array was oriented such that the angle $\bar{\alpha}$ was roughly 90°. Taking the separation Δ y=3 meters limits the phase analysis to waves larger than 6 meters. For the wind driven sea of 9 August the shortest wave length considered in this analysis is about 10 meters.

As can be seen from Figures 10 and 11 the 65% confidence interval is very large for low frequencies, decreases for the wind driven sea and then widens again. This is explained as follows: For the low and high frequency ends of the curve coherence decreases thus causing a large error in the phase angles. For the low frequency end this error is larger or of the same order as the phase angle itself. As the propagation velocity decreases with the increasing frequency the cross-spectral phase angles increase while the error $\Delta\Theta$ remains constant for a given coherence. It is then not possible to pick a certain minimum acceptable coherence value without

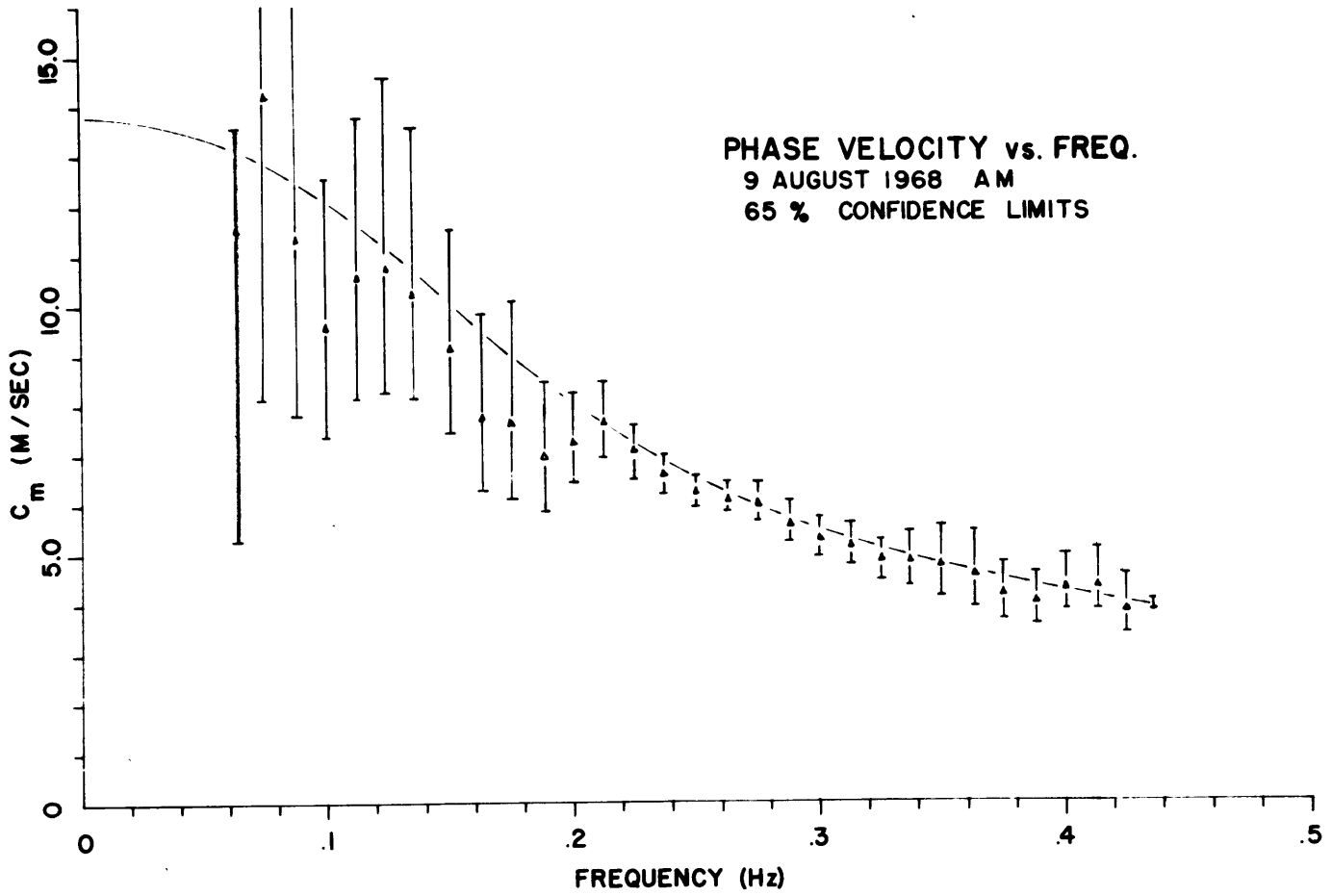

FIG. 10 PHASE SPEED 9 AUG. AM

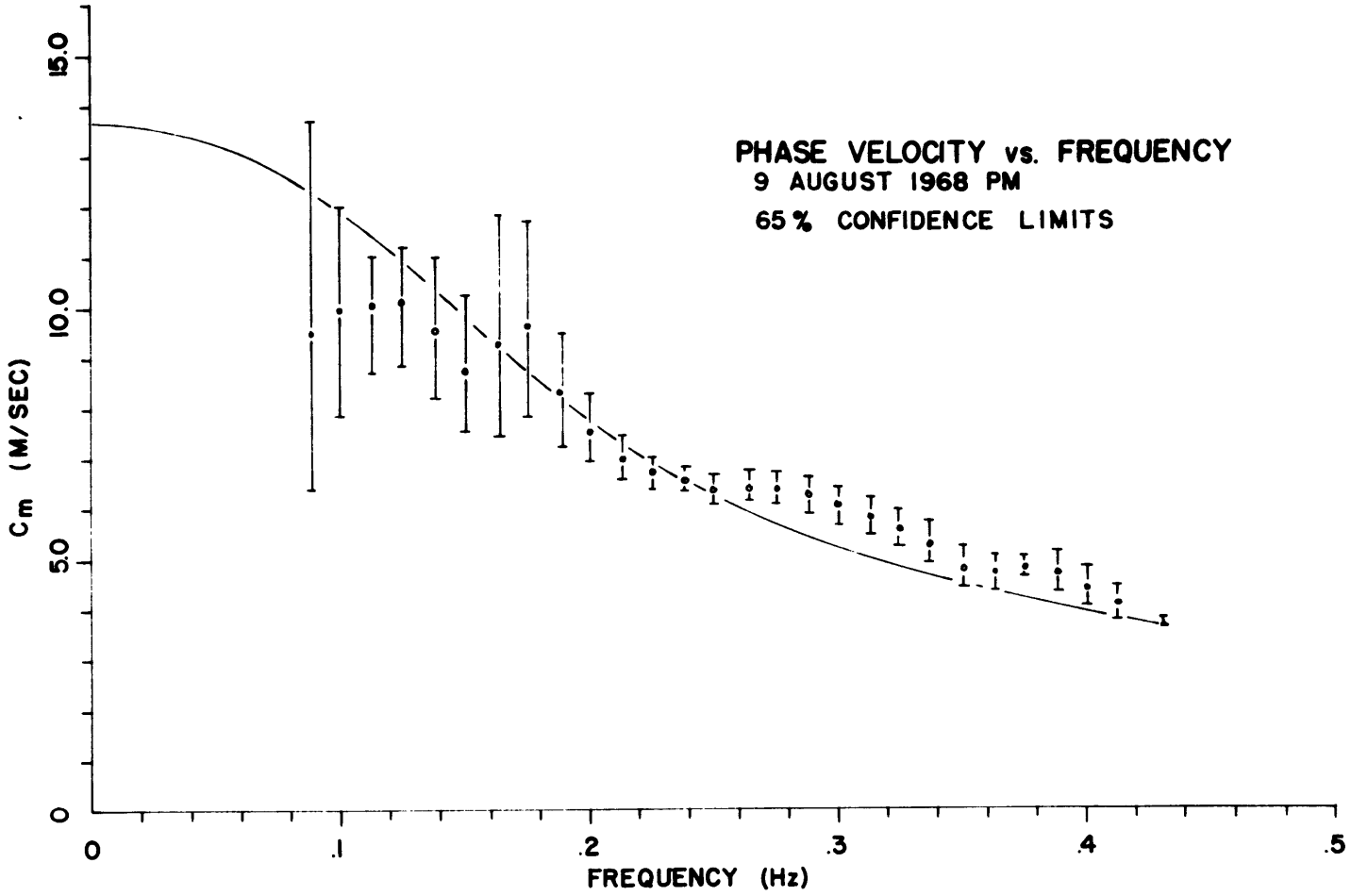

FIG. 11 PHASE SPEED 9 AUG. PM

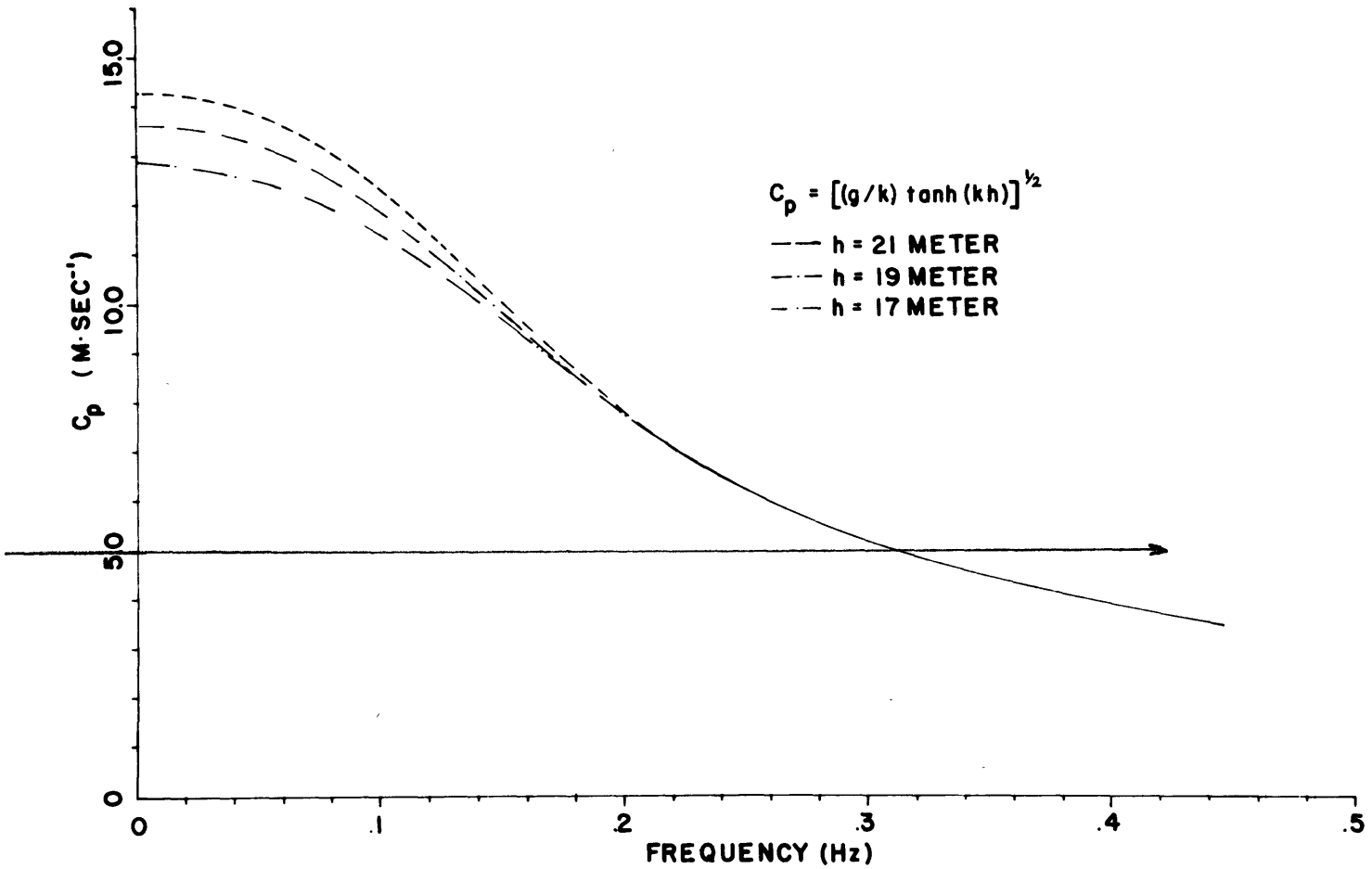

FIG. 12 THEORETICAL PHASE SPEED

cutting off either the low or high frequency end of the curves. The low frequency cut off for the curves chosen was as that frequency at which phase angles θ_{23} (since wave gauge pair 23 was orientated roughly in the direction of propagation) becomes larger than its error. For the upper end a coherence cut off of $\gamma^2 = .1$ was chosen.

The discussion which is to follow applies this only to the results within the frequency range set by the low and high cut off frequencies.

a. Phase speed analysis of the 9 August AM record.

For the AM record the wind eddy convection velocity $U_c = 25u_* =$ 5.05 m/sec corresponds to the theoretical phase speed of a wave with frequency near .310 hz. Waves of frequencies higher than .310 hz propagate more slowly than the eddy convection velocity and, if wind speed is used as the only criterion, wave generation as well as angular wave spread should be observed on the basis of the resonance theory.

With the convection velocity taken as the wind speed at a height of 1/4 wave length above the mean surface values of U_c which are lower than the theoretical phase speeds of all waves within the frequency range under consideration are obtained. No resonant wave growth is predicted for these values of U_c.

A question arises in this connection to the location of the spectral peak energy of the wind driven sea. The spectral peak of a developed sea falls near the frequency of a wave with a phase speed equal to the eddy convection velocity. For the AM spectra the peak should then occur near .310 hz but actually occurs near .240 hz.

Phillips (1958) suggested the equilibrium range to be that part of the spectrum in which the spectral curve is inversely proportional

to the fifth power in frequency. In order to determine the behaviour of the spectral curve with frequency, the AM spectrum was plotted in Figure 13 with both energy and frequency in logarithmic scales. The dashed straight line in this figure has a slope of -5.0, the solid line one of -7.5. The agreement between the spectral curve and the -7.5 slope is quite evident.

The higher frequency waves of a non-generating sea, or a sea in which the energy input from the wind is insufficient to maintain an equilibrium between dissipation and wave generation, are dissipated more quickly than low frequency waves and a spectral energy decay with a power of -7.5 in frequency, rather than the 5.0 power given by the equilibrium spectrum, might thus be expected. Since the history of the wind prior to the acquisition of the AM record is not known it must be assumed, on the basis of the above observation, that the wind sea which is actually observed is a remnant from a sea generated earlier in the day.

This conclusion supports the phase speed measurements which were obtained for 9 August AM. The measured phase speed showed no significant deviation from the speed predicted for these frequencies; wave spreading, and by implication, wave generation was then not expected. The record of 9 August AM is used to show the agreement between the linear dispersion relation and for waves of small amplitudes contained in the frequency band under consideration.

b. Phase speed analysis of the 9 August PM record.

For the 9 August PM record the measured and theoretical phase speeds diverage at frequencies above .225hz and since the observed phase speed

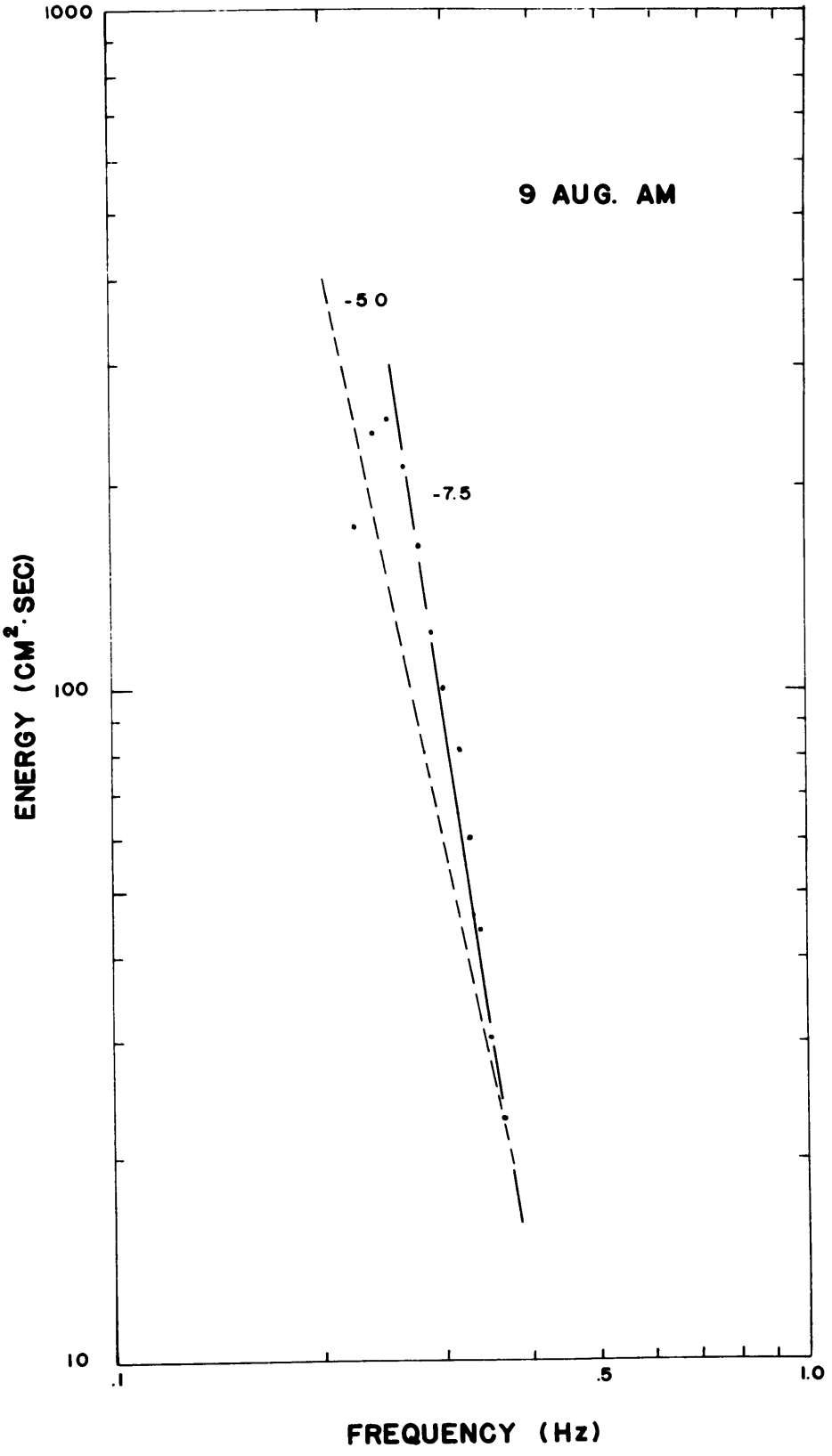

FIG. 13 LOG-LOG SPECTRUM OF 9 AUG. AM

excess is larger than the associated error bars the deviation becomes significant.

That this phase speed excess is due to wave spreading rather than nonlinear wave interactions such as found by Stokes (see Kinsman (1965)) for Longuet-Higgins and Phillips (1966) and Longuet-Higgins and Stewart (1960) is clear when we consider the measure of interaction given by the wave slope. Wave slopes encountered in these studies were less than 10^{-2}, too small to contribute significantly towards any phase speed increase.

In order to explain this observed increase in phase speed in terms of the bimodal or unimodal energy distribution it is first necessary to establish the frequency ranges of the waves undergoing Phillips or Miles wave growth. This is usually accomplished by calculating the frequency of transition from the resonant to the shear flow wave growth regime (Phillips and Katz (1961), Longuet-Higgins, Cartwright and Smith (1963)) from observations of wind speed, duration, fetch and the theory by Miles (1960).

This has unfortunately not been possible for the spectra of 9 August. That wave growth took place between the times the AM and PM wave height data were recorded is obvious from a comparison of the measured spectra. Even though the time interval between the two data runs is known, the maximum transition frequency of .350 hz found for the data of 9 August, can, at best, serve as a lower limit since Miles (1960) theory assumes the absence of any waves at the onset of wave generation by wind. This was clearly not the case for the PM spectrum.

The eddy convection velocity for 9 August PM defined as $U_c=25u_*$ is 7.2 m/sec and if resonant wave generation were to occur it should take place for waves having a frequency above .225 hz.

From the log-log plot of the PM spectrum shown in Figure 14 reasonable agreement between the dashed line with slope -5.0 and the spectral curve is noticed. It appears that the PM spectrum is near the equilibrium range. As can however be seen in Figure 14, this spectral curve is best fitted by two parallel straight lines with a slope of -5.5. These lines are offset from each other at f = .350 hz. It is thus not possible to determine the type and stage of wave generation for the PM record from available wind observations.

Measured phase speeds for this wave field indicate that wave spreading exists and, if the theory of section III were accepted, that wave generation by resonance could not take place for the following reason:

The resonance angle α = arc cos $(c_p/25u_*)$ predicts a spread phase speed c_s which is larger than the speed actually measured, even with the physically unrealistic condition that the spread of each gaussian lobe (given by σ in equation 3.15) is set to zero. If σ were not zero the phase speed c_s would even be larger. This is a consequence of $U_c > c_m$ as discussed at the end of section III.2.

The above results also apply if U_c were chosen to be the value of the wind speed 1/4 wave length above the mean sea surface.

The step in the energy spectrum shown in Figure 14 near .350 hz also shows up as an increase in observed phase speed. This step is thought to be due to wind fluctuations which were not observed over the 32 minute record for which the analysis was performed.

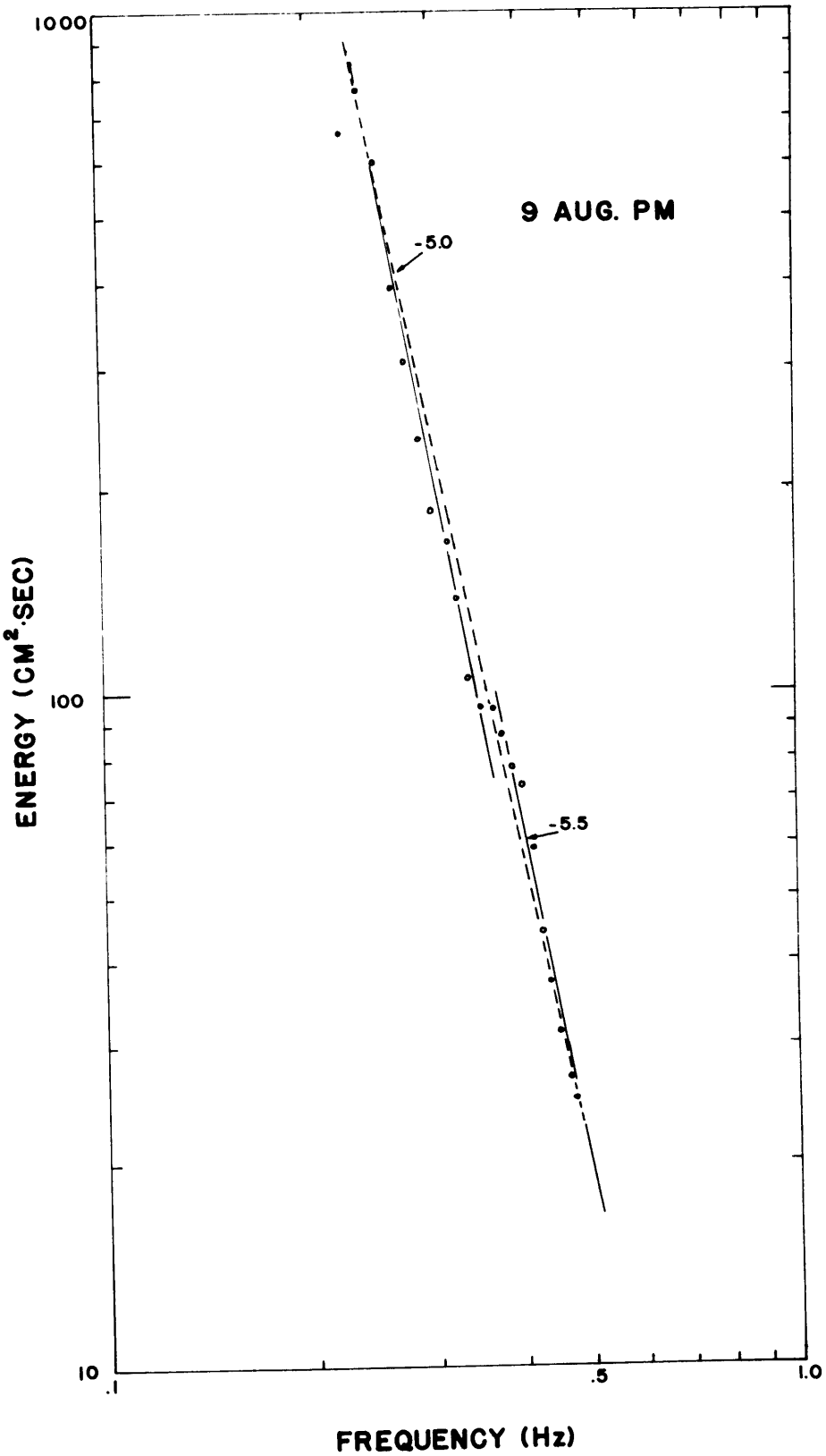

FIG. 14 LOG-LOG SPECTRUM OF 9 AUG. PM

From the above considerations we conclude that the angular energy distribution for 9 August PM is essentially unimodal ($\beta = 0$ in equation 3.15) and that the angle σ can then be calculated as a function of frequency. The values of σ are given in table III.

V.5 Two Minute Spectra

In order to explain an observed phase speed excess measured for a wave field undergoing wave generation by wind in terms of the angular energy distribution suggested by equation 3.15, it is necessary to establish the type of wave growth taking place while the wave height measurements are being collected. Since this has not been possible for the data of 9 August from the available wind information it was decided to reanalyze these records by studying their spectral development with time. This was done by dividing the record of a single wave gauge of each data run into 16 sequential two minute intervals and calculating a spectrum for each interval using the described spectral computations in section IV. Each spectrum is based on 600 data points with a digitizing interval of .2 seconds and 50 lags in the auto covariance and has a frequency range from DC to .95 hz with a resolution of .05 hz.

The results of these spectral computations are presented in matrix form in Tables IV (AM record) and VI (PM record). Columns numbered 1 through 20 list the values of energy contained by the frequency bands centered about the frequencies shown at the heading of the tables.

Two minute averages of wind speed measurements by Thornthwaite cup anemometers at 1, 2, 3, and 5 meters above the sea surface are given in columns 21 - 24 in cm/sec while column 25, the last

TABLE III

Values of σ vs. corrected frequency

for data of 9 August PM with $\beta = 0$

measured frequency	$\sigma = \arccos \frac{c_p}{c_{pm}}$
.200	--
.225	--
.250	~ 6°
.275	~26°
.300	~30°
.325	~30°
.350	~25°
.375	~30°
.400	~27°
.425	~20°

column of the tables, contains the values of the total energy expressed in cm^2, of the spectrum.

The rows of the matrices correspond to the two minute intervals which are arranged sequentially in time from n = 1 to 16. An element of the matrices presented in Tables IV and V is denoted by x_{in} where i goes from 1 to 25 and n from 1 to 16 and the following statistics were calculated using expressions given by Hoel (1963).

$$\text{Mean } \bar{x}_i = \frac{1}{N} \sum_{n=1}^{N} x_{in}$$

$$\text{Deviation} = \left[\frac{\sum_{n=1}^{N} (x_{in} - \bar{x}_n)^2}{N-1} \right]^{1/2}$$

$$\text{Linear trend} = b_i = \frac{\sum_{n=1}^{N} (2n - 2\bar{n}) x_{in}}{\sum_{n=1}^{N} (2n - 2\bar{n})^2} \qquad (5.1)$$

$$T^* = \left[\frac{(N-2) \sum_{n=1}^{N} (2n - 2\bar{n})^2}{\sum_{n=1}^{N} (x_{in} - x'_{in})^2} \right]^{1/2} \qquad (5.2)$$

$$\text{where } \bar{n} = \frac{1}{N} \sum_{n=1}^{N} n = \frac{N+1}{2}$$

The linear time regression line based on 16 observations is given by:

$$x'_{in} = 2b_i (n - \bar{n}) + \bar{x}_i \qquad (5.3)$$

The factor of 2 appearing with n and $\bar{n}$ in equations 5.1, 5.2, and 5.3 expresses the linear scale in minutes, rather than observations. The linear trend given by b_i is the slope of the line given by equation 5.3 which is fitted to the observed values by least squares.

T* is used in determining the significance levels for the regression coefficient b_i:

If the true regression coefficient is given by β' the value t' according to Hoel (1962) is:

$$t' = |b - \beta'| T^*$$

When the calculated value of t', based on the unknown true linear trend β' and the linear trend b calculated from the data, exceeds $t'_{1-\frac{\alpha}{2}}$, the value obtained from Student's distribution for a significance level of acceptance given by α and for N-2 degrees of freedom, the difference between b and β' is significant. If $t'_{1-\frac{\alpha}{2}}$ forms the upper limit of the significance level, equation 5.4 can be solved for β' and

$$b - \frac{t'_{1-\frac{\alpha}{2}}}{T^*} \leq \beta' \leq b + \frac{t'_{1-\alpha/2}}{T^*} \qquad (5.5)$$

For the 95% level of significance the value given by Student's t for 14 degrees of freedom is 2.145 and equation 5.5 becomes

$$b - \frac{2.145}{T^*} \leq \beta' \leq b + \frac{2.145}{T^*} \qquad (5.6)$$

Equation 5.6 gives the range of the true regression coefficient which could yield the value of b_i assuming 95% confidence limits. Expressed differently: What is the range of the true regression coefficient such that the measured regression coefficient will fall between $b_i - \frac{2.145}{T^*}$ and $b_i + \frac{2.145}{T^*}$ in 95 and out of 100 measurements?

The statistical analyses which were performed assume that the 16 observations are independent of each other. This condition is not fulfilled at the very low frequency components (DC - .05 hz) since the fluctuations in energy are slow compared to the two minute observations. The total energy (column 25) depends mostly on higher frequencies and the total energy estimates may be considered to be independent.

The computed results of the means, deviations, linear trends and values of T* are listed directly below the input data on Tables IV and VI.

Another valuable statistic which was computed for the input data of Tables IV and VI is r_{ij}, the linear correlation coefficient for the data of columns i and j which is defined by the relation:

$$r_{ij} = \frac{\sum_{n=1}^{N} x_{in} x_{jn} - \left(\sum_{n=1}^{N} x_{in}\right)\left(\sum_{n=1}^{N} x_{jn}\right)}{\left[\left(\sum_{n=1}^{N} (x_{in} - \bar{x}_i)^2\right)\left(\sum_{n=1}^{N} (x_{jn} - \bar{x}_j)^2\right)\right]^{1/2}} \qquad (5.7)$$

The values of r_{ij}, where the indicies i and j run from 1 to 25 (25 being the maximum number of columns of the input data) form a 25 by 25 matrix which is symmetric about its main diagonal (i=j), the elements of which are equal to 1.0.

The lower and upper 95% confidence limits for the true or population coherence ρ is given by Hoel (1962):

$$r_{\substack{u \\ L}} = \tanh\left(\frac{1}{2}\ln\frac{1+\rho}{1-\rho} \pm \frac{2}{\sqrt{N-3}}\right) \qquad (5.8)$$

The values of r_u and r_L obtained from the above equation define the range of the correlation coefficient which would be calculated in 95 out of 100 analyses for the true correlation coefficient ρ. Not all columns of the input data are however independent. Because the rough spectral energy estimates were "Hanned" to produce the final smoothed spectra, adjoining spectral components may be correlated with a measured correlation coefficient anywhere between -.5 and .8. For spectral components separated by one spectral component the measured correlation coefficient ranges from -.5 to .67. A calculated correlation coefficient between adjoining spectral bands must be outside the limits stated above in order to be significant.

The correlation matrices obtained for the data of 9 August AM and PM are presented in Tables V and VII respectively.

The indices of the columns and rows are found above to the left and right of the correlation matrices and refer to the columns of the input matrix.

We now begin with the discussion of the basic statistics for 9 August AM and PM.

a. 9 August AM

The 95% significance levels obtained from the values of T* found

TABLE IV

INPUT MATRIX FOR DATA OF ...S AUGUST AM

	FREQUENCY (HZ)																			WIND				TOTAL
	0.0	0.05	0.10	0.15	0.20	0.25	0.30	0.35	0.40	0.45	0.50	0.55	0.60	0.65	0.70	0.75	0.80	0.85	0.90	0.95	1 M	2 M	3 M	5 M	ENERGY
	1	2	3	4	5	6	7	8	9	10	11	12	13	14	15	16	17	18	19	20	21	22	23	24	25
1	61.00	78.00	97.00	74.00	39.00	46.00	69.00	62.00	31.00	21.00	24.00	23.00	16.00	8.30	7.60	6.60	3.80	3.90	5.10	5.00	238.00	167.00	277.00	299.00	34.00
2	23.00	38.00	64.00	78.00	120.00	140.00	93.00	35.00	13.00	7.70	6.00	4.20	2.70	2.20	1.60	0.94	0.54	0.48	0.64	0.75	248.00	116.00	286.00	307.00	31.00
3	25.00	31.00	45.00	53.00	89.00	150.00	120.00	49.00	23.00	16.00	11.00	7.90	4.80	4.40	4.20	3.10	3.00	3.00	2.20	1.70	240.00	260.00	280.00	296.00	32.00
4	42.00	73.00	110.00	120.00	220.00	290.00	160.00	42.00	22.00	9.80	4.00	2.10	1.60	0.92	0.72	0.59	0.31	0.07	0.09	0.07	244.00	266.00	287.00	299.00	54.00
5	26.00	48.00	72.00	64.00	90.00	140.00	97.00	33.00	20.00	11.00	4.80	3.00	1.40	0.87	0.55	0.33	0.11	0.12	0.08	0.11	235.00	255.00	274.00	286.00	30.00
6	29.00	40.00	55.00	59.00	120.00	180.00	130.00	44.00	17.00	9.70	4.00	2.40	1.20	0.78	0.67	0.50	0.30	0.15	0.13	0.18	237.00	261.00	279.00	293.00	34.00
7	16.00	49.00	83.00	72.00	150.00	240.00	150.00	52.00	29.00	19.00	9.10	3.20	1.70	1.20	0.73	0.53	0.58	0.35	0.18	0.10	243.00	267.00	286.00	295.00	44.00
8	42.00	64.00	86.00	69.00	97.00	140.00	96.00	35.00	18.00	9.30	3.80	1.90	1.70	1.10	0.64	0.56	0.50	0.33	0.20	0.15	257.00	276.00	289.00	300.00	33.00
9	21.00	52.00	87.00	85.00	140.00	220.00	180.00	97.00	42.00	16.00	5.00	1.60	1.20	1.00	0.84	0.53	0.40	0.30	0.22	0.23	268.00	298.00	314.00	328.00	47.00
10	21.00	60.00	130.00	110.00	84.00	140.00	130.00	58.00	22.00	9.70	4.40	3.50	2.30	1.50	1.10	1.20	0.81	0.70	0.58	0.51	285.00	320.00	344.00	365.00	39.00
11	37.00	43.00	52.00	48.00	120.00	220.00	140.00	43.00	19.00	7.00	3.30	2.40	1.20	1.10	1.00	0.69	0.46	0.41	0.28	0.24	300.00	337.00	356.00	374.00	37.00
12	24.00	50.00	87.00	72.00	74.00	110.00	77.00	37.00	20.00	8.30	4.40	2.60	1.50	1.10	0.80	0.77	0.74	0.42	0.18	0.15	283.00	318.00	342.00	366.00	28.00
13	12.00	38.00	61.00	51.00	58.00	73.00	67.00	45.00	22.00	10.00	5.50	3.00	1.10	1.10	0.98	0.51	0.56	0.65	0.55	0.35	271.00	303.00	327.00	349.00	23.00
14	23.00	63.00	110.00	91.00	130.00	190.00	140.00	49.00	21.00	9.90	5.80	4.20	2.40	1.60	1.40	1.30	1.20	1.00	0.85	0.77	283.00	312.00	330.00	349.00	43.00
15	34.00	39.00	44.00	41.00	48.00	61.00	56.00	39.00	25.00	14.00	5.50	1.80	1.40	0.99	0.74	0.48	0.41	0.30	0.16	0.10	279.00	302.00	321.00	343.00	20.00
16	41.00	44.00	44.00	49.00	87.00	150.00	150.00	81.00	22.00	7.20	5.20	3.00	1.60	1.10	0.84	0.84	0.67	0.40	0.38	0.38	274.00	302.00	324.00	342.00	34.00
	MEAN																				MEAN				
	29.81	50.63	76.69	71.00	104.12	155.62	115.94	50.06	22.87	11.60	6.61	4.36	2.74	1.83	1.53	1.22	0.90	0.79	0.74	0.67	261.56	272.62	307.25	324.44	35.19
	DEVIATION																				DEVIATION				
	12.36	13.50	26.41	22.23	44.61	66.41	37.35	17.49	6.67	4.29	5.04	5.19	3.65	1.93	1.84	1.58	1.02	1.08	1.27	1.23	21.17	57.53	27.77	30.59	8.73
	DEVIATION / MEAN																				DEVIATION / MEAN				
	0.41	0.27	0.34	0.31	0.43	0.43	0.32	0.35	0.29	0.37	0.76	1.19	1.33	1.06	1.20	1.30	1.13	1.37	1.72	1.82	0.08	0.21	0.09	0.09	0.25
	LINEAR TREND																				LINEAR TREND				
	-0.32	-0.30	-0.40	-0.68	-1.10	-0.89	0.04	0.34	0.01	-0.18	-0.26	-0.27	-0.19	-0.11	-0.10	-0.08	-0.04	-0.05	-0.06	-0.06	1.80	4.66	2.30	2.46	-0.22
	T STAR																				T STAR				
	2.57	2.70	1.36	1.68	0.82	0.54	0.95	2.07	5.34	9.06	8.09	7.90	11.28	21.88	22.69	25.65	38.51	36.76	31.67	33.10	2.87	0.97	2.09	1.81	4.20

TABLE V

CORRELATION COEFFICIENTS FOR DATA OF....9 AUGUST AM

	1	2	3	4	5	6	7	8	9	10	11	12	13	14	15	16	17	18	19	20	21	22	23	24	25	
1	1.000	0.552	0.019	-0.015	-0.117	-0.153	-0.129	0.056	0.030	0.145	0.494	0.580	0.627	0.536	0.530	0.575	0.429	0.413	0.542	0.576	-0.164	-0.265	-0.231	-0.207	0.069	1
2	0.552	1.000	0.812	0.692	0.225	0.136	0.124	0.123	0.250	0.213	0.352	0.422	0.475	0.330	0.307	0.395	0.244	0.215	0.364	0.403	-0.084	-0.087	-0.103	-0.111	0.545	2
3	0.019	0.812	1.000	0.901	0.302	0.230	0.224	0.090	0.196	0.099	0.094	0.152	0.188	0.093	0.067	0.148	0.065	0.039	0.117	0.140	0.056	0.044	0.086	0.071	0.588	3
4	-0.015	0.692	0.901	1.000	0.582	0.463	0.416	0.107	0.122	-0.010	-0.042	0.011	0.051	-0.009	-0.030	0.024	-0.045	-0.074	-0.012	0.012	-0.082	-0.091	-0.047	-0.066	0.741	4
5	-0.117	0.225	0.302	0.582	1.000	0.951	0.767	0.043	0.020	-0.147	-0.378	-0.407	-0.387	-0.396	-0.393	-0.396	-0.394	-0.425	-0.423	-0.411	-0.182	0.024	-0.176	-0.257	0.846	5
6	-0.153	0.136	0.230	0.463	0.951	1.000	0.882	0.153	0.087	-0.134	-0.410	-0.446	-0.435	-0.431	-0.420	-0.418	-0.387	-0.420	-0.452	-0.450	-0.064	0.206	-0.052	-0.151	0.855	6
7	-0.129	0.124	0.224	0.416	0.767	0.882	1.000	0.554	0.309	-0.047	-0.296	-0.326	-0.320	-0.311	-0.293	-0.273	-0.235	-0.270	-0.308	-0.307	0.037	0.279	0.056	-0.036	0.854	7
8	0.056	0.123	0.090	0.107	0.043	0.153	0.554	1.000	0.762	0.325	0.198	0.149	0.158	0.143	0.159	0.185	0.172	0.157	0.180	0.187	0.141	0.157	0.161	0.142	0.391	8
9	0.030	0.250	0.196	0.122	0.020	0.087	0.309	0.762	1.000	0.730	0.379	0.257	0.278	0.248	0.261	0.269	0.248	0.248	0.270	0.266	-0.022	0.132	-0.014	-0.034	0.346	9
10	0.145	0.213	0.099	-0.010	-0.147	-0.134	-0.047	0.325	0.730	1.000	0.762	0.610	0.615	0.622	0.619	0.603	0.604	0.610	0.609	0.591	-0.459	-0.282	-0.457	-0.442	0.121	10
11	0.494	0.352	0.094	-0.042	-0.378	-0.410	-0.296	0.198	0.379	0.762	1.000	0.969	0.962	0.957	0.949	0.949	0.891	0.896	0.956	0.956	-0.420	-0.539	-0.408	-0.340	-0.049	11
12	0.580	0.422	0.152	0.011	-0.407	-0.446	-0.326	0.149	0.257	0.610	0.969	1.000	0.995	0.977	0.971	0.982	0.898	0.907	0.986	0.994	-0.355	-0.539	-0.341	-0.265	-0.061	12
13	0.627	0.475	0.188	0.051	-0.387	-0.435	-0.320	0.158	0.278	0.615	0.962	0.995	1.000	0.974	0.964	0.979	0.884	0.890	0.979	0.991	-0.349	-0.547	-0.346	-0.271	-0.034	13
14	0.536	0.330	0.093	-0.009	-0.396	-0.431	-0.311	0.143	0.248	0.622	0.957	0.977	0.974	1.000	0.997	0.991	0.952	0.960	0.992	0.986	-0.363	-0.560	-0.359	-0.281	-0.074	14
15	0.530	0.307	0.067	-0.030	-0.393	-0.420	-0.293	0.159	0.261	0.619	0.949	0.971	0.964	0.997	1.000	0.991	0.963	0.972	0.993	0.983	-0.346	-0.519	-0.339	-0.262	-0.072	15
16	0.575	0.395	0.148	0.024	-0.396	-0.418	-0.273	0.185	0.269	0.603	0.949	0.982	0.979	0.991	0.991	1.000	0.956	0.958	0.995	0.990	-0.305	-0.473	-0.296	-0.221	-0.035	16
17	0.429	0.244	0.065	-0.045	-0.394	-0.387	-0.235	0.172	0.248	0.604	0.891	0.898	0.884	0.952	0.963	0.956	1.000	0.995	0.949	0.918	-0.275	-0.370	-0.265	-0.197	-0.064	17
18	0.413	0.215	0.039	-0.074	-0.425	-0.420	-0.270	0.157	0.248	0.610	0.896	0.907	0.890	0.960	0.972	0.958	0.995	1.000	0.959	0.928	-0.288	-0.392	-0.277	-0.206	-0.103	18
19	0.542	0.364	0.117	-0.012	-0.423	-0.452	-0.308	0.180	0.270	0.609	0.956	0.986	0.979	0.992	0.993	0.995	0.949	0.959	1.000	0.995	-0.314	-0.496	-0.306	-0.229	-0.074	19
20	0.576	0.403	0.140	0.012	-0.411	-0.450	-0.307	0.187	0.266	0.591	0.956	0.994	0.991	0.986	0.983	0.990	0.918	0.928	0.995	1.000	-0.318	-0.534	-0.312	-0.234	-0.059	20
21	-0.164	-0.084	0.056	-0.082	-0.182	-0.064	0.037	0.141	-0.022	-0.459	-0.420	-0.355	-0.349	-0.363	-0.346	-0.305	-0.275	-0.288	-0.314	-0.318	1.000	0.686	0.980	0.969	-0.112	21
22	-0.265	-0.087	0.044	-0.091	0.024	0.206	0.279	0.157	0.132	-0.282	-0.539	-0.539	-0.547	-0.560	-0.519	-0.473	-0.370	-0.392	-0.496	-0.534	0.686	1.000	0.707	0.640	0.068	22
23	-0.231	-0.103	0.086	-0.047	-0.176	-0.052	0.056	0.161	-0.014	-0.457	-0.408	-0.341	-0.346	-0.359	-0.339	-0.296	-0.265	-0.277	-0.306	-0.312	0.980	0.707	1.000	0.992	-0.094	23
24	-0.207	-0.111	0.071	-0.066	-0.257	-0.151	-0.036	0.142	-0.034	-0.442	-0.340	-0.265	-0.271	-0.281	-0.262	-0.221	-0.197	-0.206	-0.229	-0.234	0.969	0.640	0.992	1.000	-0.169	24
25	0.069	0.545	0.588	0.741	0.846	0.855	0.854	0.391	0.346	0.121	-0.049	-0.061	-0.034	-0.074	-0.072	-0.035	-0.064	-0.103	-0.074	-0.059	-0.112	0.068	-0.094	-0.169	1.000	25

TABLE VI

INPUT MATRIX FOR DATA OF ...9 AUGUST PM

	FREQUENCY (HZ)																				WIND				TOTAL
	0.0	0.05	0.10	0.15	0.20	0.25	0.30	0.35	0.40	0.45	0.50	0.55	0.60	0.65	0.70	0.75	0.80	0.85	0.90	0.95	1 M	2 M	3 M	5 M	ENERGY
	1	2	3	4	5	6	7	8	9	10	11	12	13	14	15	16	17	18	19	20	21	22	23	24	25
1	29.00	72.00	130.00	140.00	230.00	270.00	170.00	97.00	51.00	19.00	9.60	7.30	6.10	3.70	2.50	1.40	0.65	0.40	0.35	0.18	428.00	460.00	482.00	507.00	61.00
2	9.30	54.00	120.00	140.00	230.00	300.00	180.00	68.00	40.00	27.00	17.00	9.60	6.10	4.50	2.60	1.30	0.58	0.47	0.36	0.14	418.00	462.00	491.00	518.00	61.00
3	14.00	50.00	83.00	140.00	370.00	440.00	210.00	87.00	55.00	25.00	16.00	8.60	5.40	3.50	2.60	1.50	1.00	0.67	0.41	0.27	448.00	493.00	521.00	542.00	75.00
4	23.00	46.00	76.00	110.00	350.00	500.00	240.00	77.00	86.00	52.00	18.00	7.70	5.10	2.70	1.90	1.00	0.73	0.60	0.36	0.17	435.00	472.00	507.00	532.00	80.00
5	36.00	62.00	100.00	130.00	240.00	310.00	190.00	87.00	49.00	32.00	25.00	14.00	8.00	4.20	2.20	0.93	0.54	0.36	0.25	0.10	430.00	468.00	496.00	529.00	63.00
6	14.00	51.00	110.00	150.00	310.00	390.00	240.00	130.00	81.00	31.00	11.00	4.60	3.70	2.50	1.80	1.20	1.00	1.10	0.68	0.16	416.00	453.00	479.00	509.00	77.00
7	33.00	62.00	110.00	150.00	250.00	300.00	220.00	140.00	70.00	37.00	24.00	8.10	5.40	4.00	2.00	1.00	0.84	0.73	0.60	0.42	417.00	458.00	489.00	515.00	71.00
8	38.00	49.00	48.00	86.00	340.00	460.00	230.00	75.00	68.00	48.00	22.00	7.20	5.00	3.10	1.80	1.30	1.10	0.74	0.72	0.57	423.00	457.00	477.00	503.00	74.00
9	19.00	45.00	92.00	150.00	320.00	390.00	230.00	85.00	45.00	26.00	15.00	11.00	7.50	3.10	1.20	1.00	0.87	0.42	0.31	0.28	434.00	469.00	495.00	520.00	72.00
10	23.00	50.00	83.00	100.00	150.00	260.00	230.00	150.00	70.00	33.00	17.00	6.20	4.40	3.20	2.20	1.20	0.95	0.76	0.63	0.40	433.00	472.00	497.00	515.00	61.00
11	28.00	63.00	100.00	98.00	180.00	340.00	330.00	150.00	86.00	47.00	24.00	14.00	8.00	5.20	3.50	1.60	0.86	0.49	0.31	0.23	440.00	483.00	509.00	523.00	76.00
12	35.00	58.00	94.00	120.00	420.00	700.00	410.00	100.00	55.00	33.00	17.00	9.50	5.90	3.50	2.30	1.50	1.30	1.30	0.99	0.58	437.00	474.00	500.00	521.00	100.00
13	11.00	34.00	58.00	81.00	310.00	530.00	360.00	140.00	63.00	29.00	20.00	15.00	7.60	4.20	3.50	2.60	1.90	2.00	2.00	2.00	421.00	455.00	481.00	513.00	84.00
14	28.00	41.00	54.00	62.00	270.00	490.00	330.00	110.00	72.00	48.00	28.00	14.00	6.50	3.90	2.00	1.10	0.61	0.35	0.36	0.34	444.00	479.00	508.00	530.00	78.00
15	23.00	49.00	86.00	110.00	250.00	430.00	260.00	130.00	58.00	44.00	13.00	7.00	5.10	3.00	1.90	1.70	1.70	0.96	0.55	0.39	413.00	452.00	483.00	511.00	78.00
16	35.00	71.00	120.00	130.00	230.00	390.00	320.00	140.00	70.00	38.00	23.00	20.00	13.00	6.40	4.10	5.40	7.80	8.40	5.20	2.70	435.00	470.00	500.00	529.00	84.00
	MEAN																				MEAN				
	24.89	53.56	91.50	118.56	283.13	406.25	259.37	112.87	66.19	35.56	18.72	10.24	6.42	3.79	2.38	1.61	1.40	1.23	0.88	0.56	429.50	467.31	494.69	519.81	74.69
	DEVIATION																				DEVIATION				
	9.38	10.46	24.19	27.32	67.20	115.17	69.71	34.06	16.37	9.76	5.28	4.10	2.17	0.99	0.75	1.09	1.75	1.96	1.23	0.73	10.56	11.57	12.59	10.53	10.30
	DEVIATION / MEAN																				DEVIATION / MEAN				
	0.38	0.20	0.26	0.23	0.24	0.28	0.27	0.30	0.25	0.27	0.28	0.40	0.34	0.26	0.32	0.68	1.25	1.59	1.39	1.30	0.02	0.02	0.03	0.02	0.14
	LINEAR TREND																				LINEAR TREND				
	0.24	-0.22	-0.88	-1.53	-0.20	4.85	5.67	1.95	0.78	0.44	0.21	0.22	0.10	0.03	0.02	0.06	0.10	0.10	0.07	0.05	0.07	-0.03	0.01	-0.02	0.63
	T STAR																				T STAR				
	3.92	3.48	1.57	1.54	0.53	0.34	0.81	1.26	2.44	4.05	7.27	10.07	18.17	38.05	49.67	38.41	24.06	20.95	34.16	61.11	3.38	3.08	2.83	3.39	4.26

TABLE VII

CORRELATION COEFFICIENTS FOR DATA OF....9 AUGUST PM

	1	2	3	4	5	6	7	8	9	10	11	12	13	14	15	16	17	18	19	20	21	22	23	24	25	
1	1.000	0.545	C.C06	-C.149	-C.C74	0.060	0.162	C.061	0.104	0.396	C.470	0.215	C.287	0.246	0.007	0.132	C.234	C.220	0.192	C.C93	0.170	0.048	0.001	-0.042	C.152	1
2	C.545	1.000	C.795	C.494	-0.423	-C.433	-0.202	0.163	-0.134	-0.193	-C.C15	C.151	C.351	C.512	0.344	C.301	0.342	C.346	0.268	C.C47	C.C36	C.C57	C.028	-0.006	-C.193	2
3	0.006	0.795	1.000	C.789	-C.4C9	-0.524	-0.335	C.106	-0.253	-0.506	-0.357	C.CC2	C.249	0.353	0.224	C.199	0.224	C.244	0.166	-C.C46	-0.197	-C.11C	-0.073	-C.046	-C.293	3
4	-C.149	C.494	C.789	1.000	0.027	-0.376	-0.521	-0.221	-0.382	-0.611	-C.493	-0.253	-0.0C2	-0.038	-0.165	-0.034	0.045	0.061	-0.014	-C.193	-0.221	-C.115	-C.072	0.026	-0.251	4
5	-C.074	-C.423	-C.4C9	0.C27	1.000	C.824	0.271	-0.514	-0.072	0.015	-C.242	-C.263	-C.3C5	-0.522	-0.359	-C.153	-C.124	-C.119	-0.094	-0.C36	0.121	0.061	0.065	0.138	C.648	5
6	C.060	-C.433	-C.524	-C.376	C.824	1.000	C.735	-C.184	C.121	C.278	C.065	C.1C6	-C.032	-0.196	-0.020	C.C95	C.075	C.082	C.132	C.234	C.237	C.137	C.150	C.177	C.9CC	6
7	C.162	-C.2C2	-C.335	-C.521	C.271	C.735	1.000	C.446	C.285	C.336	C.33C	C.478	C.326	C.266	C.411	C.40C	C.34C	C.35C	C.4C8	C.5C9	C.278	C.185	C.187	C.122	C.859	7
8	C.061	C.163	C.1C6	-C.221	-C.514	-C.184	C.446	1.00C	C.559	C.200	C.159	C.252	C.220	C.383	C.494	C.329	C.276	C.27C	C.285	C.319	-C.030	C.015	C.016	-C.132	C.151	8
9	C.1C4	-C.134	-C.253	-C.382	-C.072	C.121	C.285	C.559	1.CCC	C.734	C.C65	-C.139	-C.167	-C.142	C.029	C.1CC	C.135	C.C99	C.C7C	C.C52	-C.151	-C.132	-C.024	-C.1C4	C.3C3	9
10	C.396	-C.193	-C.506	-C.611	C.C15	C.278	C.336	C.20C	C.734	1.000	C.540	C.102	-C.CC9	C.000	-C.C52	C.CC7	C.C72	C.043	C.020	C.C07	C.090	C.077	C.171	C.1C2	C.323	10
11	C.47C	-C.C15	-C.357	-C.493	-C.242	C.065	C.33C	C.199	C.C65	C.540	1.CCC	C.636	C.436	C.528	C.277	C.153	C.163	C.174	C.199	C.247	C.312	C.3C9	C.341	C.371	C.112	11
12	C.215	C.151	C.CC2	-C.253	-C.263	C.106	C.478	C.252	-C.139	C.1C2	C.636	1.CCC	C.528	C.844	C.69C	C.676	C.619	C.624	C.646	C.679	C.364	C.285	C.310	C.437	C.26C	12
13	C.287	C.391	C.249	-C.CC2	-C.3C5	-C.C32	C.326	C.22C	-C.167	-C.CC9	C.436	C.928	1.CCC	C.872	C.694	C.8C1	C.78C	C.775	C.768	C.722	C.283	C.196	C.217	C.345	C.189	13
14	C.246	C.512	C.353	-C.C38	-C.522	-C.196	C.286	C.383	-C.142	C.000	C.528	C.844	C.872	1.000	C.845	C.724	C.659	C.666	C.664	C.617	C.211	C.232	C.242	C.286	C.052	14
15	C.CC7	C.344	C.224	-C.165	-C.359	-C.C2C	C.411	C.494	C.029	-C.052	C.277	C.69C	C.694	C.845	1.000	C.776	C.638	C.656	C.687	C.709	C.19C	C.2C7	C.197	C.219	C.2C8	15
16	C.132	C.3C1	C.199	-C.C34	-C.153	C.095	C.400	C.329	C.100	C.CC7	C.153	C.676	C.8C1	C.724	C.776	1.000	C.972	C.969	C.974	C.921	C.068	-C.CC7	C.023	C.137	C.362	16
17	C.234	C.342	C.224	C.C45	-C.124	C.075	C.340	C.276	C.135	C.072	C.163	C.619	C.78C	C.659	C.638	C.972	1.00C	C.994	C.976	C.871	C.063	-C.C17	C.034	C.156	C.356	17
18	C.220	C.346	C.244	C.C61	-C.119	C.082	C.350	C.27C	C.099	C.043	C.174	C.624	C.775	C.666	C.656	C.969	C.994	1.CCC	C.988	C.882	C.C61	-C.C22	C.C29	C.161	C.363	18
19	C.192	C.268	C.166	-C.C14	-C.094	C.132	C.408	C.285	C.070	C.020	C.199	C.646	C.768	C.664	C.687	C.974	C.976	C.988	1.000	C.942	C.C29	-C.C65	-C.031	C.106	C.392	19
20	C.C93	C.C47	-C.046	-C.193	-C.C36	C.234	C.509	C.219	C.C52	C.007	C.247	C.679	C.722	C.617	C.7C9	C.921	C.871	C.882	C.942	1.CCC	-C.011	-C.126	-C.103	C.033	C.436	20
21	C.170	C.C36	-C.197	-C.221	C.121	C.237	C.278	-C.C3C	-C.151	C.09C	C.312	C.364	C.283	C.211	C.150	C.068	C.063	C.C61	C.C29	-C.C11	1.CCC	C.945	C.875	C.759	C.2C6	21
22	C.048	C.C57	-C.110	-C.115	C.061	C.137	C.189	C.C15	-C.132	C.C77	C.309	C.285	C.196	C.232	C.207	-C.CC7	-C.017	-C.022	-C.C69	-C.126	C.945	1.CCC	C.959	C.825	C.126	22
23	C.CC1	C.C28	-C.C73	-C.C72	C.C65	C.15C	C.187	C.016	-C.024	C.171	C.341	C.31C	C.217	C.242	C.157	C.023	C.034	C.C29	-C.031	-C.103	C.875	C.959	1.CCC	C.921	C.166	23
24	-C.C42	-C.CC6	-C.C46	C.C26	C.138	C.177	C.122	-C.132	-C.104	C.102	C.371	C.437	C.345	C.286	C.219	C.137	C.156	C.161	C.106	C.C33	C.759	C.825	C.921	1.CCC	C.181	24
25	C.152	-C.193	-C.293	-C.251	C.648	C.900	C.859	C.151	C.3C3	C.323	C.112	C.26C	C.189	C.052	C.2C8	C.362	C.356	C.363	C.392	C.436	C.2C6	C.126	C.168	C.181	1.CCC	25

for the frequencies of .50 - .95 hz (columns 10 to 20) are sufficiently narrow to establish that the linear trends of the spectral energies at these frequencies are slightly negative, implying that energy of higher frequency waves is being dissipated very slowly. No definite conclusion can be drawn about the sign of the linear trends of the other variables since their small values of T* produce significance limits which are larger than the measured linear trends.

It should be mentioned that the measure of linear trend is used in this study to determine changes of either spectral energy or wind speed with time, linear trend can however not be used to determine the change of the quantities as a function of time.

In order to proceed with the analysis it is necessary to consider the correlation coefficients given in Table V next. It may be stated at this time that, while the correlation coefficients are often not larger than the 95% significance limits for a zero true correlation coefficient, the consistent grouping of signs of the correlation coefficient is thought to be of significance.

Correlation coefficients found for the submatrix formed by frequencies between .50 - .95 hz (columns 11 to 20) are all positive and significantly different from zero, indicating that the frequencies between .50 and .95 hz are undergoing the same process. The correlation between the above frequencies and the total energy (column 25) is low but consistingly negative.

The frequency range .20 to .45 hz (columns 5 to 10) includes the bulk of the spectral energy and the spectral components correlate highly, as was expected, with total energy. Spectral components between .20 and .45 hz correlate poorly but negatively with each other.

All spectral frequency components with the exception of columns 7 and 8 correlate negatively with the wind speeds given in column 21 to 24. It is of interest to note that, even though the correlation coefficient is low, wind and the frequencies of .30 -.35 hz correlate positively and that the theoretical phase speed of waves of .30 -.35 hz is near the eddy convection velocity $U_c = 25\ u_*$.

The conclusion which can be drawn from these observation is that the spectrum of 9 August AM is not undergoing wave generation by wind but that waves with a frequency between .50 and .95 hz are actually decaying with time. Whether the energy lost by the higher frequencies is transferred to lower frequency waves can not be determined. Support to the above conclusion is lent by the two previous observations, namely the steep decay of the spectral curve with frequency and the fact that no phase speed excess was observed.

The conclusion that the spectrum of 9 August AM is of a decaying sea and that the measured phase velocity agrees with the linear dispersion relation appears to be very reasonable.

b. 9 August PM

While a comparison between the AM and PM spectra clearly shows that wave generation by wind has taken place, the question whether wave generation is still taking place has not been answered.

The linear trend of the total energy of the PM spectrum has a value of .63 $\pm$ .50 and can be considered positive, that is wave generation is still active. All frequency components, with the exception of the swell, were found to correlate positively with energy, the correlation coefficient being high for the frequencies containing the spectral peak (.20 - .30 hz) and low with the frequencies between .55 and .95 hz. Values of linear trend obtained for .30 and .35 hz indicate that wave growth is still active at these frequencies and, while waves of frequencies above .45 hz are highly intercorrelated, they have slightly positive but insignificant linear trends. The higher frequency components appear to have ceased wave growth while waves of frequency near the spectral peak are still growing in height.

It may be mentioned that these frequency components correlate negatively with frequency components just below the spectral peak, but positively with frequency components just above the spectral peak. Since the correlation coefficients do however not extend over the significance levels and since the linear trend of the frequency component just below the spectral peak has a very large uncertainty, no conclusion concerning interaction between these spectral areas can be drawn.

The wind speeds have an uncertain linear trends, correlate poorly with the high frequencies even though the correlation coefficients generally increase with anemometer height.

The above observations indicate that wave generation is still

taking place, even if very slowly, for waves near the spectral peak. Waves of frequencies above .45 hz are saturated and do not grow any higher. This conclusion agrees well with the observed phase speed excess, there exists wave spreading for waves near .30 - .35 hz but the spread decreases in width with frequency as expected from the above considerations.

VI. Summary

VI.1 Angular energy distribution $\Phi(k,\xi)$

The results of this investigation are insufficient and not well enough defined to either accept or reject the idea and specific form of the angular energy distribution suggested on physical grounds in section III. Direct proof of the existance of such energy distribution by directional spectral analysis appears to be unlikely. While the effect of wave spreading upon phase speed measurements of the wave field has been demonstrated theoretically, its application to phase speeds obtained in this investigation from actual wave height measurements was inconlusive. A comparison of phase speed measurements of waves undergoing wave growth by clearly identifiable wave generation mechanisms with the phase speed predicted by the appropriate angular energy distribution should be able to prove or disprove the angular energy distribution suggested by equation 3.15.

VI.2 Directional spectral analysis

A computational investigation of directional analysis performed on several theoretical wave fields was undertaken. The results showed that the resolution which can be obtained for the wave gauge array used in this investigation is too poor to be of value in determining the validity of the suggested angular energy distribution.

VI.3 Phase speed analysis

The method of cross-spectral analysis of wave height information used in this study proved to be successful as was demonstrated for the data of 9 August AM. Waves of this record were found to propagate as predicted by potential wave theory.

Phase speed measurements for 9 August PM exceed the values given by the dispersion relation. An estimation of the maximum slope from the energy spectrum indicates that this phase speed excess should be explained in terms of wave spread rather than nonlinear interactions.

VI.4 Analysis of Wave Generation

Because of the uncertain initial conditions of wind and sea state, efforts to determine the mechanism of wave generation active on the wave field from wind observations proved to be fruitless.

Some success was however achieved by the analyses of short spectra as a function of time. The analyses established the existence of wave growth for some frequency components. An application of spectral time series analysis to developing spectra should be able to establish the regions of Miles and Phillips' wave growth within a spectrum. Since the 9 August PM spectrum appears to be very close to an equilibrium spectrum, the active regime could not be identified.

VI.5 Correlation coefficients

With the presence of a direct common cause (such as a source of energy) it is not possible to indicate any linear interdependency between observed quantities on basis of correlation coefficients since these coefficients reflect the response of these quantities to the common cause. Correlation coefficients serve us as a convenient tool to map out regions of the observed quantities having similar behaviour or response.

In a closed system (where there is no direct commone cause acting on the quantities) the correlation coefficient of the observed quantities may describe their linear dependency. The difficulty lies, however, in determining that there is no common cause acting directly on all observed quantities.

For the spectral analysis performed in section V there exist two direct common causes which make the interpretation of the correlation coefficients in terms of nonlinear interactions unsuitable. For 9 August AM there exists dissipation of wave energy. Since it is not clear however that this dissipation is due to nonlinear interaction only, no conclusions can be drawn from the correlation coefficients with regard to linear dependency of frequency components. Since the observed phase speed is essentially equal to the phase speed given by the linear dispersion relation, the waves are actually considered to be independent of each other.

The wind acts as a source of energy for the waves observed in the 9 August PM record. There can thus be no explanation of linear dependency in terms of the correlation coefficient since a group of waves may simply behave similiarly under the influence of wind.

Appendix

On 14 August 1968 Drs. Garret and Barger covered an area of the sea surface upwind of the spar with an artificial slick in order to observe its effect on the wave field. The deployment of the slick as well as some of its gross effects on air sea interactions are described by Barger et al. (1969). Measurements of wave height and the wind field above the waves were obtained by Ruggles (1969) before, during and after the slick's presence at the spar.

Since wave height was measured at two points only the data are unsuitable for wave phase speed calculations; the original wave height data were however redigitized and analyzed by the author in terms of two minute spectra in an attempt to study the effect of the slick on the waves more thoroughly.

Prior to subdividing the three records wave energy spectra were calculated for the whole 32 minute records as described in section IV, the resulting energy spectra are shown in figure 1A. The resulting sequential two minute wave energy spectra for the three records are presented in matrix form, along with two minute wind speed and total energy averages as discussed in section V.5, in Table IA through IIIA. Correlation coefficients between the variables of these tables are found in tables IVA through VIA. Since the angle between the current and the mean direction of main propagation is not known the frequency correction cannot be applied to these spectra.

As can be seen from figure 1A, the wave energy spectra observed before and during the slick's presence at the spar are very similar

but for a shift of the wind driven sea peak energy to a higher frequency during the presence of the slick. Analysis of this shift in frequency in terms of two minute spectra is of no help because of the relatively poor resolution of the short spectra.

During the last quarter of the slick wave height measurements the wind speed increased and it began to rain, there was however no shift in wind direction. This increase in wind speed shows up as a fairly large and statistically signifcant linear trend on Table IIA, the change of wind speed is however not reflected in the spectral energies for the frequency range which was analyzed. Since the duration of higher wind speeds is relatively short and a slick is present, it is impossible to draw any conclusions about the wave generation mechanism which may or may not exist under these conditions. The combination of these two factors yields the observed spectrum.

The wave spectrum observed one hour after the slick's presence shows a large increase in the energy of the wind driven sea. Since the slick did not cover the whole wave generation area, the observed spectrum must be that of an advected sea.

The analysis of the correlation coefficients does not appear to contribute significantly to our understanding of the processes involved in the wave generation. This may be due to the fact that we are analyzing frequencies which are too low for the effect of surface tension to be noticed or, that the spectra are already well established by the time the data were obtained. It should be remembered that a zero correlation coefficient does not infer that var-

iables are independent of each other and conversely that a non zero, even if significant, correlation coefficient does not infer that the variables are dependent on each other.

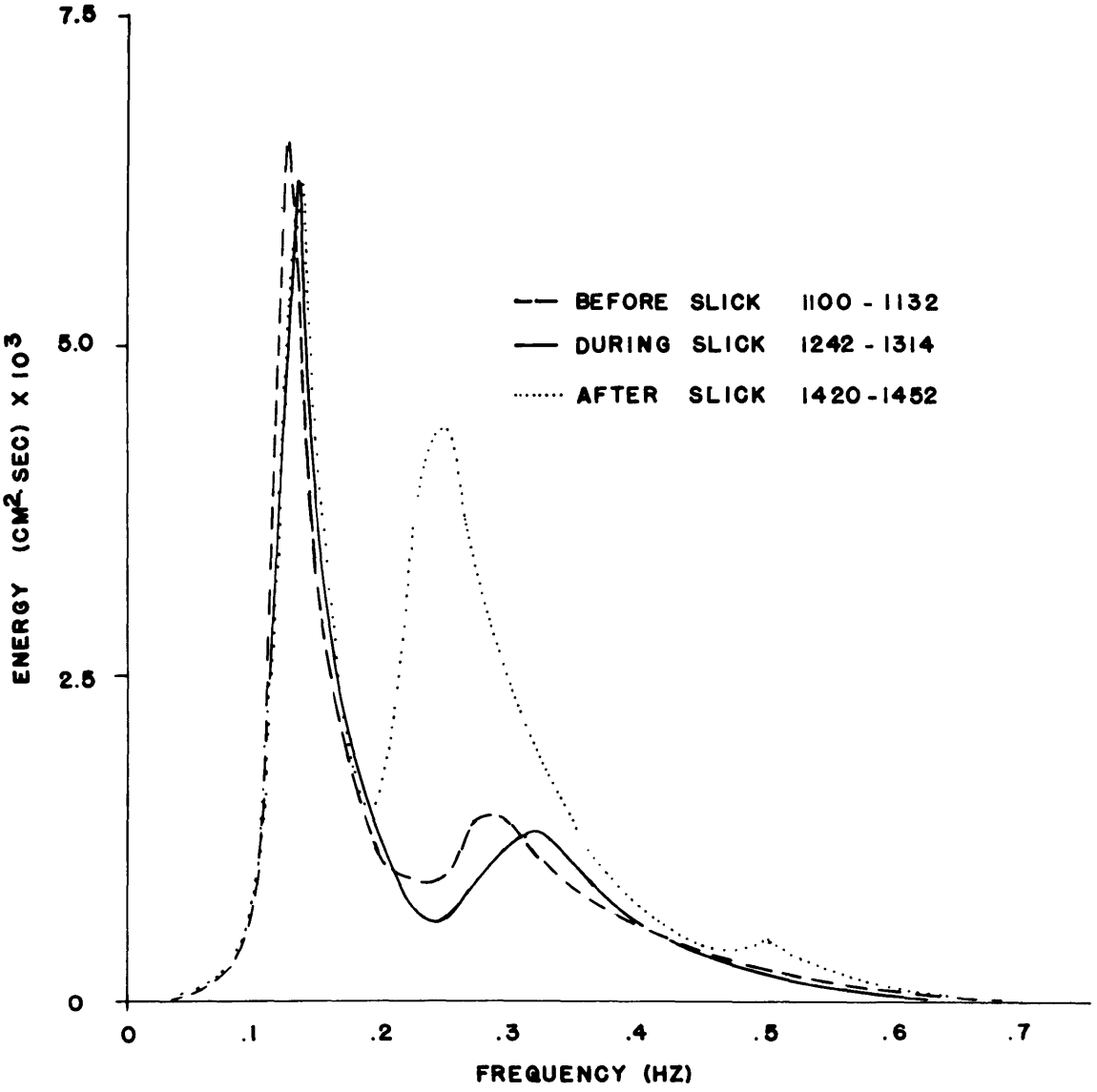

FIG. 1A WAVE ENERGY SPECTRA OF 14 AUG. 1968

TABLE IA

INPUT MATRIX FOR DATA OF ...14 AUGUST BEFORE SLICK

	FREQUENCY (HZ)																				WIND			TOTAL
	0.0	0.05	0.10	0.15	0.20	0.25	0.30	0.35	0.40	0.45	0.50	0.55	0.60	0.65	0.70	0.75	0.80	0.85	0.90	0.95	1 M	2 M	3 M	5 M	ENERGY
	1	2	3	4	5	6	7	8	9	10	11	12	13	14	15	16	17	18	19	20	21	22	23	24	25
1	30.00	410.00	2300.00	2900.00	1300.00	700.00	850.00	680.00	470.00	260.00	220.00	220.00	150.00	70.00	47.00	52.00	46.00	31.00	14.00	7.10	414.00	448.00	485.00	484.00	540.00
2	67.00	570.00	2600.00	3300.00	1800.00	1300.00	1400.00	1100.00	660.00	440.00	310.00	220.00	160.00	100.00	74.00	49.00	37.00	29.00	23.00	14.00	396.00	433.00	469.00	468.00	720.00
3	180.00	830.00	4100.00	4900.00	2100.00	880.00	1100.00	1000.00	770.00	530.00	350.00	180.00	110.00	56.00	33.00	28.00	28.00	23.00	21.00	18.00	401.00	449.00	489.00	485.00	850.00
4	39.00	240.00	1700.00	2600.00	1400.00	740.00	1300.00	1400.00	770.00	300.00	190.00	150.00	100.00	88.00	84.00	53.00	32.00	28.00	21.00	11.00	426.00	469.00	503.00	500.00	560.00
5	22.00	370.00	2100.00	2900.00	1600.00	880.00	840.00	730.00	550.00	290.00	210.00	170.00	120.00	110.00	91.00	48.00	25.00	26.00	28.00	18.00	433.00	475.00	508.00	503.00	560.00
6	20.00	300.00	1500.00	2200.00	1500.00	1200.00	1400.00	1400.00	1000.00	570.00	310.00	190.00	160.00	130.00	98.00	66.00	41.00	36.00	26.00	15.00	426.00	470.00	506.00	508.00	620.00
7	81.00	390.00	1600.00	2800.00	2400.00	1400.00	1100.00	770.00	480.00	400.00	350.00	210.00	93.00	91.00	97.00	63.00	28.00	22.00	24.00	22.00	422.00	466.00	504.00	502.00	630.00
8	15.00	250.00	1700.00	2900.00	2200.00	1600.00	1400.00	970.00	530.00	440.00	340.00	170.00	100.00	110.00	90.00	52.00	32.00	25.00	27.00	24.00	426.00	476.00	508.00	502.00	650.00
9	110.00	720.00	3800.00	4500.00	1800.00	1000.00	1200.00	840.00	380.00	130.00	140.00	150.00	140.00	120.00	91.00	60.00	36.00	24.00	26.00	18.00	446.00	489.00	526.00	503.00	770.00
10	26.00	170.00	1200.00	2100.00	1600.00	1300.00	1400.00	1000.00	710.00	450.00	230.00	150.00	110.00	110.00	91.00	43.00	20.00	17.00	18.00	16.00	421.00	461.00	496.00	499.00	540.00
11	32.00	290.00	1700.00	2400.00	1300.00	790.00	860.00	640.00	500.00	370.00	190.00	97.00	88.00	84.00	74.00	56.00	42.00	28.00	21.00	15.00	422.00	467.00	502.00	504.00	480.00
12	85.00	350.00	2100.00	3000.00	1700.00	1200.00	1500.00	810.00	440.00	410.00	310.00	220.00	120.00	77.00	62.00	47.00	35.00	28.00	22.00	14.00	410.00	458.00	496.00	496.00	630.00
13	44.00	170.00	560.00	1100.00	1300.00	930.00	500.00	410.00	410.00	310.00	200.00	180.00	140.00	84.00	71.00	39.00	21.00	16.00	10.00	6.20	436.00	480.00	519.00	517.00	330.00
14	100.00	570.00	2700.00	3200.00	1700.00	1300.00	1200.00	940.00	660.00	370.00	270.00	220.00	120.00	67.00	68.00	66.00	45.00	24.00	16.00	11.00	417.00	466.00	503.00	512.00	680.00
15	20.00	430.00	1900.00	2600.00	1500.00	920.00	1200.00	910.00	520.00	360.00	200.00	130.00	120.00	82.00	52.00	44.00	40.00	35.00	20.00	10.00	427.00	474.00	509.00	513.00	560.00
16	41.00	540.00	2200.00	2800.00	1700.00	1100.00	1400.00	1500.00	920.00	350.00	230.00	140.00	64.00	58.00	51.00	48.00	53.00	46.00	27.00	13.00	430.00	475.00	511.00	504.00	670.00
	MEAN																				MEAN				
	57.00	412.50	2110.00	2887.50	1681.25	1077.50	1165.62	943.75	610.63	373.75	253.12	174.81	118.44	89.81	73.38	50.88	35.06	27.37	21.50	14.52	422.06	466.00	502.13	500.00	611.88
	DEVIATION																				DEVIATION				
	44.75	190.21	889.19	880.81	325.00	261.50	277.94	295.47	183.10	106.20	66.71	37.29	26.77	21.94	19.89	10.10	9.30	7.36	5.07	4.88	12.60	13.83	13.44	12.24	120.79
	LINEAR TREND																				LINEAR TREND				
	-0.63	-2.75	-25.26	-30.59	-4.63	4.91	1.60	-1.78	-1.65	-1.24	-1.86	-1.45	-1.18	-0.53	-0.22	0.04	0.21	0.12	-0.06	-0.10	0.55	0.80	0.81	0.92	-3.26
	T STAR																				T STAR				
	0.80	0.19	0.04	0.04	0.11	0.14	0.13	0.12	0.20	0.34	0.55	1.03	1.47	1.67	1.80	3.53	3.92	4.90	7.07	7.44	3.11	3.09	3.23	4.19	0.31

TABLE IIA

INPUT MATRIX FOR DATA OF ...14 AUGUST DURING SLICK

	FREQUENCY (HZ)													FREQUENCY (HZ)							WIND				TOTAL
	0.0	0.05	0.10	0.15	0.20	0.25	0.30	0.35	0.40	0.45	0.50	0.55	0.60	0.65	0.70	0.75	0.80	0.85	0.90	0.95	1 M	2 M	3 M	5 M	ENERGY
	1	2	3	4	5	6	7	8	9	10	11	12	13	14	15	16	17	18	19	20	21	22	23	24	25
1	25.00	89.00	760.00	1900.00	1900.00	1300.00	1200.00	1000.00	650.00	310.00	170.00	140.00	86.00	50.00	38.00	29.00	25.00	23.00	18.00	14.00	419.00	464.00	540.00	501.00	490.00
2	31.00	290.00	2100.00	3200.00	2100.00	1200.00	1300.00	1500.00	1000.00	440.00	330.00	230.00	110.00	70.00	42.00	37.00	36.00	31.00	20.00	11.00	405.00	445.00	488.00	473.00	710.00
3	140.00	500.00	3500.00	5000.00	2600.00	1100.00	1100.00	1100.00	860.00	480.00	400.00	350.00	170.00	44.00	27.00	19.00	20.00	25.00	25.00	16.00	398.00	436.00	465.00	470.00	870.00
4	1.10	240.00	1000.00	1700.00	1500.00	1100.00	1100.00	1100.00	630.00	220.00	190.00	200.00	140.00	110.00	87.00	52.00	35.00	25.00	20.00	18.00	388.00	422.00	464.00	455.00	490.00
5	17.00	170.00	1400.00	3100.00	2800.00	1300.00	780.00	930.00	780.00	540.00	380.00	260.00	160.00	110.00	73.00	52.00	41.00	28.00	15.00	11.00	388.00	432.00	450.00	457.00	650.00
6	74.00	420.00	2000.00	3100.00	1900.00	1100.00	1700.00	1600.00	880.00	610.00	400.00	190.00	120.00	72.00	67.00	65.00	44.00	28.00	24.00	17.00	367.00	404.00	450.00	427.00	720.00
7	52.00	350.00	2400.00	4000.00	2700.00	1100.00	930.00	920.00	530.00	360.00	330.00	200.00	110.00	82.00	59.00	47.00	39.00	35.00	33.00	27.00	363.00	400.00	418.00	422.00	710.00
8	84.00	680.00	2700.00	3700.00	2000.00	870.00	1100.00	1000.00	630.00	400.00	220.00	120.00	110.00	88.00	72.00	53.00	28.00	18.00	17.00	12.00	380.00	424.00	416.00	443.00	700.00
9	65.00	690.00	3100.00	4100.00	2100.00	1100.00	1300.00	740.00	390.00	370.00	310.00	250.00	150.00	65.00	40.00	42.00	34.00	22.00	18.00	14.00	387.00	425.00	440.00	448.00	750.00
10	36.00	360.00	2100.00	3000.00	1600.00	840.00	1000.00	840.00	500.00	280.00	180.00	140.00	140.00	91.00	73.00	76.00	63.00	41.00	24.00	16.00	413.00	452.00	445.00	478.00	570.00
11	81.00	390.00	2300.00	3300.00	1800.00	760.00	620.00	500.00	370.00	200.00	110.00	110.00	90.00	82.00	68.00	46.00	37.00	31.00	22.00	13.00	434.00	474.00	470.00	500.00	550.00
12	4.10	430.00	1900.00	2400.00	1200.00	670.00	840.00	740.00	430.00	200.00	87.00	72.00	77.00	80.00	67.00	40.00	23.00	15.00	14.00	10.00	449.00	493.00	487.00	521.00	470.00
13	41.00	360.00	2100.00	3000.00	1700.00	830.00	880.00	830.00	600.00	330.00	210.00	170.00	130.00	94.00	81.00	58.00	32.00	34.00	39.00	35.00	528.00	570.00	513.00	597.00	580.00
14	13.00	230.00	920.00	1500.00	1500.00	1100.00	1200.00	1200.00	680.00	330.00	260.00	120.00	79.00	42.00	43.00	45.00	27.00	20.00	21.00	16.00	615.00	673.00	583.00	705.00	470.00
15	0.20	290.00	1600.00	2400.00	1600.00	1000.00	1300.00	1300.00	740.00	280.00	140.00	92.00	83.00	83.00	59.00	44.00	37.00	26.00	21.00	18.00	649.00	712.00	695.00	749.00	560.00
16	42.00	370.00	2000.00	2800.00	1600.00	1200.00	1700.00	1600.00	890.00	440.00	250.00	170.00	120.00	110.00	97.00	68.00	42.00	25.00	20.00	18.00	618.00	670.00	687.00	701.00	680.00
	MEAN															MEAN									
	44.15	365.50	1992.50	3012.50	1912.50	1035.62	1128.12	1056.25	660.00	361.88	247.94	175.87	117.19	79.56	62.06	48.31	35.19	26.69	21.94	16.62	450.06	493.50	500.69	521.69	623.13
	DEVIATION															DEVIATION									
	37.63	161.39	751.14	922.23	458.80	189.31	298.33	318.37	189.03	118.78	101.32	72.22	29.47	21.79	19.50	14.33	10.22	6.68	6.38	6.37	96.42	103.53	85.94	106.49	117.68
	LINEAR TREND															LINEAR TREND									
	-0.96	2.94	-1.38	-22.21	-26.62	-9.70	1.51	-1.66	-5.41	-4.04	-4.77	-4.35	-1.13	0.55	0.88	0.67	0.17	-0.05	0.09	0.18	7.88	8.41	5.22	8.41	-3.80
	T STAR															T STAR									
	0.98	0.22	0.05	0.04	0.09	0.22	0.12	0.11	0.20	0.32	0.39	0.60	1.30	1.68	2.03	2.78	3.53	5.34	5.64	5.81	0.59	0.54	0.51	0.51	0.32

TABLE IIIA

INPUT MATRIX FOR DATA OF ...14 AUGUST AFTER SLICK

	FREQUENCY (HZ)																				WIND			TOTAL
	0.0	0.05	0.10	0.15	0.20	0.25	0.30	0.35	0.40	0.45	0.50	0.55	0.60	0.65	0.70	0.75	0.80	0.85	0.90	0.95	1 M	2 M	3 M	5 M	ENERGY
	1	2	3	4	5	6	7	8	9	10	11	12	13	14	15	16	17	18	19	20	21	22	23	24	25
1	40.00	340.00	2300.00	3500.00	3800.00	4800.00	3600.00	1800.00	1100.00	530.00	360.00	240.00	140.00	110.00	84.00	75.00	49.00	36.00	35.00	27.00	438.00	487.00	514.00	512.00	1100.00
2	75.00	350.00	2300.00	3800.00	5100.00	6500.00	4300.00	1800.00	860.00	480.00	430.00	290.00	170.00	120.00	120.00	80.00	31.00	20.00	24.00	20.00	440.00	490.00	515.00	527.00	1300.00
3	1.20	250.00	970.00	1700.00	2600.00	3000.00	2400.00	1500.00	940.00	480.00	200.00	130.00	150.00	130.00	89.00	54.00	29.00	24.00	29.00	26.00	420.00	469.00	497.00	501.00	740.00
4	6.70	470.00	2600.00	3800.00	2900.00	2900.00	2900.00	1700.00	770.00	410.00	250.00	230.00	210.00	130.00	72.00	37.00	24.00	31.00	31.00	21.00	410.00	472.00	500.00	510.00	980.00
5	29.00	210.00	2100.00	4300.00	4400.00	3600.00	2400.00	1600.00	850.00	300.00	250.00	150.00	91.00	95.00	77.00	39.00	24.00	24.00	21.00	22.00	456.00	512.00	543.00	542.00	1000.00
6	11.00	230.00	1300.00	2500.00	3500.00	4300.00	3000.00	1200.00	670.00	470.00	340.00	320.00	210.00	89.00	50.00	58.00	52.00	32.00	20.00	16.00	471.00	519.00	548.00	551.00	920.00
7	17.00	230.00	1600.00	3100.00	3100.00	3200.00	2900.00	1600.00	660.00	410.00	310.00	200.00	180.00	160.00	97.00	48.00	36.00	34.00	25.00	16.00	457.00	513.00	540.00	546.00	910.00
8	60.00	290.00	2100.00	3400.00	2500.00	2100.00	2100.00	1200.00	580.00	440.00	270.00	180.00	170.00	100.00	63.00	46.00	37.00	29.00	22.00	17.00	456.00	502.00	528.00	543.00	780.00
9	27.00	220.00	1000.00	2000.00	2300.00	2600.00	2500.00	1500.00	640.00	440.00	290.00	190.00	170.00	120.00	59.00	33.00	35.00	32.00	19.00	18.00	450.00	509.00	536.00	534.00	720.00
10	21.00	250.00	1300.00	2100.00	2300.00	2200.00	1800.00	1300.00	740.00	420.00	400.00	250.00	110.00	87.00	59.00	41.00	31.00	29.00	30.00	21.00	447.00	502.00	526.00	517.00	680.00
11	110.00	600.00	3000.00	3900.00	3100.00	3500.00	3000.00	1600.00	760.00	500.00	450.00	260.00	110.00	96.00	77.00	55.00	46.00	36.00	34.00	32.00	489.00	545.00	570.00	570.00	1100.00
12	11.00	250.00	920.00	1500.00	2300.00	2700.00	1900.00	1200.00	1100.00	750.00	480.00	300.00	160.00	110.00	74.00	48.00	41.00	32.00	22.00	21.00	505.00	563.00	601.00	610.00	700.00
13	21.00	390.00	2300.00	3600.00	2800.00	2500.00	2300.00	1500.00	920.00	650.00	510.00	360.00	190.00	87.00	54.00	37.00	46.00	46.00	22.00	8.10	509.00	558.00	587.00	605.00	920.00
14	95.00	290.00	1700.00	3100.00	2700.00	2500.00	2100.00	1300.00	770.00	480.00	300.00	180.00	180.00	160.00	90.00	48.00	31.00	28.00	24.00	13.00	515.00	575.00	602.00	605.00	800.00
15	5.60	300.00	1400.00	2100.00	2400.00	2900.00	2200.00	1300.00	830.00	460.00	360.00	230.00	110.00	92.00	71.00	43.00	32.00	25.00	19.00	15.00	522.00	582.00	611.00	614.00	750.00
16	11.00	180.00	1400.00	2800.00	2900.00	2600.00	1800.00	920.00	470.00	230.00	220.00	220.00	120.00	60.00	44.00	34.00	37.00	34.00	20.00	14.00	510.00	569.00	602.00	612.00	710.00
	MEAN																				MEAN				
	33.84	303.13	1768.12	2950.00	3043.75	3243.75	2575.00	1438.75	791.25	465.62	338.75	233.12	154.44	109.12	73.75	48.50	36.31	30.75	24.81	19.19	468.44	522.94	551.25	556.19	881.88
	DEVIATION																				DEVIATION				
	33.47	108.73	630.72	871.01	801.64	1133.12	682.64	247.17	172.47	119.27	94.22	62.58	37.30	26.87	19.50	13.55	8.48	6.15	5.32	5.90	35.51	37.26	38.91	40.68	179.15
	LINEAR TREND																				LINEAR TREND				
	0.13	-0.89	-15.90	-26.47	-49.78	-74.78	-51.03	-18.46	-5.78	0.54	2.12	1.14	-0.85	-0.90	-1.02	-0.84	0.09	0.20	-0.25	-0.32	3.29	3.55	3.67	3.75	-10.90
	T STAR																				T STAR				
	1.07	0.33	0.06	0.04	0.06	0.04	0.07	0.20	0.22	0.30	0.39	0.58	0.98	1.40	2.11	3.26	4.22	6.11	7.47	7.02	2.14	2.27	2.08	1.83	0.24

TABLE IV A

CORRELATION COEFFICIENTS FOR DATA OF....14 AUGUST BEFORE SLICK

	1	2	3	4	5	6	7	8	9	10	11	12	13	14	15	16	17	18	19	20	21	22	23	24	25	
1	1.000	0.786	0.770	0.766	0.477	-0.006	0.045	-0.058	-0.042	0.073	0.318	0.309	0.013	-0.397	-0.382	-0.224	-0.083	-0.276	-0.043	0.180	-0.372	-0.255	-0.149	-0.297	0.686	1
2	0.786	1.000	0.943	0.890	0.391	-0.087	0.133	0.150	0.087	-0.082	0.138	0.166	0.070	-0.341	-0.476	-0.109	0.329	0.191	0.225	0.141	-0.273	-0.220	-0.156	-0.379	0.833	2
3	0.770	0.943	1.000	0.973	0.355	-0.141	0.189	0.136	0.027	-0.134	0.087	0.127	0.087	-0.237	-0.403	-0.103	0.260	0.104	0.274	0.225	-0.269	-0.221	-0.179	-0.445	0.860	3
4	0.766	0.890	0.973	1.000	0.516	-0.026	0.270	0.148	-0.003	-0.074	0.204	0.135	0.006	-0.167	-0.302	-0.095	0.156	0.043	0.382	0.407	-0.285	-0.218	-0.187	-0.474	0.904	4
5	0.477	0.391	0.355	0.516	1.000	0.669	0.370	0.107	-0.019	0.300	0.704	0.295	-0.273	0.038	0.149	0.034	-0.205	-0.175	0.483	0.804	-0.211	-0.079	-0.064	-0.216	0.653	5
6	-0.006	-0.087	-0.141	-0.026	0.669	1.000	0.566	0.183	0.093	0.449	0.641	0.355	-0.064	0.319	0.427	0.293	-0.108	-0.139	0.316	0.570	-0.140	-0.029	-0.052	0.001	0.289	6
7	0.045	0.133	0.189	0.270	0.370	0.566	1.000	0.742	0.477	0.401	0.388	0.096	-0.125	0.183	0.134	0.191	0.255	0.373	0.525	0.358	-0.271	-0.182	-0.226	-0.244	0.573	7
8	-0.058	0.150	0.136	0.148	0.107	0.183	0.742	1.000	0.870	0.355	0.183	-0.098	-0.200	0.058	0.040	0.157	0.385	0.617	0.490	0.106	-0.105	-0.073	-0.116	-0.134	0.448	8
9	-0.042	0.087	0.027	-0.003	-0.019	0.093	0.477	0.870	1.000	0.582	0.263	-0.065	-0.132	-0.016	-0.039	0.032	0.273	0.498	0.288	0.005	-0.200	-0.169	-0.190	-0.075	0.291	9
10	0.073	-0.082	-0.134	-0.074	0.300	0.449	0.401	0.355	0.582	1.000	0.782	0.194	-0.012	0.011	-0.042	-0.156	-0.095	0.061	0.121	0.273	-0.586	-0.446	-0.446	-0.180	0.205	10
11	0.318	0.138	0.087	0.204	0.704	0.641	0.388	0.183	0.263	0.782	1.000	0.583	-0.011	-0.082	-0.035	-0.031	-0.095	-0.046	0.220	0.486	-0.639	-0.491	-0.471	-0.354	0.441	11
12	0.309	0.166	0.127	0.135	0.295	0.355	0.096	-0.098	-0.065	0.194	0.583	1.000	0.511	-0.089	-0.050	0.157	-0.026	-0.175	-0.197	-0.064	-0.500	-0.515	-0.464	-0.396	0.235	12
13	0.013	0.070	0.087	0.006	-0.273	-0.064	-0.125	-0.200	-0.132	-0.012	-0.011	0.511	1.000	0.410	0.100	0.104	-0.083	-0.173	-0.267	-0.317	-0.148	-0.277	-0.251	-0.270	-0.018	13
14	-0.397	-0.341	-0.237	-0.167	0.038	0.319	0.183	0.058	-0.016	0.011	-0.082	-0.089	0.410	1.000	0.860	0.397	-0.345	-0.197	0.418	0.418	0.400	0.306	0.240	0.104	-0.072	14
15	-0.382	-0.476	-0.403	-0.302	0.149	0.427	0.134	0.040	-0.039	-0.042	-0.035	-0.050	0.100	0.860	1.000	0.587	-0.380	-0.307	0.375	0.473	0.451	0.388	0.325	0.260	-0.181	15
16	-0.224	-0.109	-0.103	-0.095	0.034	0.293	0.191	0.157	0.032	-0.156	-0.031	0.157	0.104	0.397	0.587	1.000	0.418	0.178	0.256	0.148	0.281	0.249	0.219	0.256	0.029	16
17	-0.083	0.329	0.260	0.156	-0.205	-0.108	0.255	0.385	0.273	-0.095	-0.095	-0.026	-0.083	-0.345	-0.380	0.418	1.000	0.816	0.148	-0.284	-0.080	-0.072	-0.080	-0.042	0.236	17
18	-0.276	0.191	0.104	0.043	-0.175	-0.139	0.373	0.617	0.498	0.061	-0.046	-0.175	-0.173	-0.197	-0.307	0.178	0.816	1.000	0.432	-0.171	-0.000	-0.003	-0.037	-0.041	0.195	18
19	-0.043	0.225	0.274	0.382	0.483	0.316	0.525	0.490	0.288	0.121	0.220	-0.197	-0.267	0.418	0.375	0.256	0.148	0.432	1.000	0.738	0.156	0.206	0.140	-0.102	0.529	19
20	0.180	0.141	0.225	0.407	0.804	0.570	0.358	0.106	0.005	0.273	0.486	-0.064	-0.317	0.418	0.473	0.148	-0.284	-0.171	0.738	1.000	0.020	0.119	0.078	-0.116	0.501	20
21	-0.372	-0.273	-0.269	-0.285	-0.211	-0.140	-0.271	-0.105	-0.200	-0.586	-0.639	-0.500	-0.148	0.400	0.451	0.281	-0.080	-0.000	0.156	0.020	1.000	0.952	0.934	0.754	-0.362	21
22	-0.255	-0.220	-0.221	-0.218	-0.079	-0.029	-0.182	-0.073	-0.169	-0.446	-0.491	-0.515	-0.277	0.306	0.388	0.249	-0.072	-0.003	0.206	0.119	0.952	1.000	0.988	0.853	-0.265	22
23	-0.149	-0.156	-0.179	-0.187	-0.064	-0.052	-0.226	-0.116	-0.190	-0.446	-0.471	-0.464	-0.251	0.240	0.325	0.219	-0.080	-0.037	0.140	0.078	0.934	0.988	1.000	0.859	-0.245	23
24	-0.297	-0.379	-0.445	-0.474	-0.216	0.001	-0.244	-0.134	-0.075	-0.180	-0.354	-0.396	-0.270	0.104	0.260	0.256	-0.042	-0.041	-0.102	-0.116	0.754	0.853	0.859	1.000	-0.466	24
25	0.686	0.833	0.860	0.904	0.653	0.289	0.573	0.448	0.291	0.205	0.441	0.235	-0.018	-0.072	-0.181	0.029	0.236	0.195	0.529	0.501	-0.362	-0.265	-0.245	-0.466	1.000	25

TABLE VA

CORRELATION COEFFICIENTS FOR DATA OF....14 AUGUST DURING SLICK

	1	2	3	4	5	6	7	8	9	10	11	12	13	14	15	16	17	18	19	20	21	22	23	24	25	
1	1.000	0.618	0.813	0.833	0.484	-0.074	0.035	-0.080	0.066	0.408	0.449	0.509	0.427	-0.337	-0.311	-0.218	-0.163	0.074	0.239	0.013	-0.394	-0.399	-0.403	-0.404	0.765	1
2	0.618	1.000	0.839	0.664	0.062	-0.428	0.100	-0.185	-0.272	0.119	0.124	0.132	0.257	-0.062	-0.049	0.044	-0.101	-0.232	-0.004	-0.068	-0.248	-0.251	-0.356	-0.274	0.561	2
3	0.813	0.839	1.000	0.937	0.403	-0.281	-0.028	-0.185	-0.096	0.256	0.339	0.453	0.455	-0.134	-0.222	-0.137	-0.051	0.101	0.224	0.045	-0.328	-0.335	-0.387	-0.350	0.802	3
4	0.833	0.664	0.937	1.000	0.688	-0.050	-0.091	-0.170	0.012	0.426	0.530	0.622	0.565	-0.122	-0.284	-0.199	-0.015	0.218	0.255	0.059	-0.467	-0.470	-0.477	-0.481	0.890	4
5	0.484	0.062	0.403	0.688	1.000	0.504	-0.159	-0.044	0.243	0.604	0.748	0.740	0.548	-0.091	-0.355	-0.307	-0.025	0.256	0.151	0.025	-0.518	-0.509	-0.449	-0.511	0.707	5
6	-0.074	-0.428	-0.281	-0.050	0.504	1.000	0.478	0.546	0.621	0.578	0.627	0.554	0.288	-0.128	-0.275	-0.206	-0.013	-0.015	-0.170	-0.103	-0.057	-0.049	0.175	-0.033	0.293	6
7	0.035	0.100	-0.028	-0.091	-0.159	0.478	1.000	0.856	0.606	0.501	0.353	0.115	0.005	-0.132	-0.021	0.196	0.121	-0.180	-0.118	-0.040	0.259	0.259	0.440	0.260	0.304	7
8	-0.080	-0.185	-0.185	-0.170	-0.044	0.546	0.856	1.000	0.884	0.579	0.432	0.160	-0.023	-0.021	0.045	0.152	0.105	-0.067	-0.060	-0.021	0.300	0.303	0.473	0.307	0.263	8
9	0.066	-0.272	-0.096	0.017	0.243	0.621	0.606	0.884	1.000	0.706	0.577	0.413	0.187	-0.042	-0.076	-0.051	-0.014	0.013	-0.035	-0.064	0.165	0.169	0.336	0.179	0.400	9
10	0.408	0.119	0.256	0.426	0.604	0.578	0.501	0.579	0.706	1.000	0.891	0.613	0.481	-0.066	-0.124	0.086	0.105	0.056	0.021	-0.049	-0.227	-0.221	-0.130	-0.229	0.721	10
11	0.449	0.124	0.339	0.530	0.748	0.627	0.353	0.432	0.577	0.891	1.000	0.825	0.618	-0.188	-0.309	-0.084	0.050	0.149	0.154	0.047	-0.360	-0.358	-0.305	-0.362	0.777	11
12	0.509	0.132	0.453	0.622	0.740	0.554	0.115	0.160	0.413	0.613	0.825	1.000	0.841	-0.128	-0.345	-0.306	-0.071	0.181	0.146	0.045	-0.440	-0.448	-0.350	-0.438	0.757	12
13	0.427	0.257	0.455	0.565	0.548	0.288	0.005	-0.023	0.187	0.481	0.618	0.841	1.000	0.238	0.045	0.107	0.237	0.309	0.154	0.114	-0.439	-0.450	-0.420	-0.448	0.624	13
14	-0.337	-0.062	-0.134	-0.122	-0.091	-0.128	-0.132	-0.021	-0.042	-0.066	-0.188	-0.128	0.238	1.000	0.908	0.663	0.508	0.272	0.011	0.174	0.014	0.005	0.022	-0.009	-0.126	14
15	-0.311	-0.049	-0.222	-0.284	-0.355	-0.275	-0.021	0.045	-0.076	-0.124	-0.309	-0.345	0.045	0.908	1.000	0.792	0.465	0.187	0.094	0.266	0.173	0.161	0.132	0.144	-0.277	15
16	-0.218	0.044	-0.137	-0.199	-0.307	-0.206	0.196	0.152	-0.051	0.086	-0.084	-0.306	0.107	0.663	0.792	1.000	0.801	0.429	0.185	0.257	0.128	0.118	0.037	0.094	-0.139	16
17	-0.163	-0.101	-0.051	-0.015	-0.025	-0.013	0.121	0.105	-0.014	0.105	0.050	-0.071	0.237	0.508	0.465	0.801	1.000	0.735	0.148	0.095	-0.061	-0.068	-0.058	-0.081	0.014	17
18	0.074	-0.232	0.101	0.218	0.256	-0.015	-0.180	-0.067	0.013	0.056	0.149	0.181	0.309	0.272	0.187	0.429	0.735	1.000	0.639	0.477	-0.149	-0.163	-0.181	-0.168	0.141	18
19	0.239	-0.004	0.224	0.255	0.151	-0.170	-0.118	-0.060	-0.035	0.021	0.154	0.146	0.154	0.011	0.094	0.185	0.148	0.639	1.000	0.928	0.071	0.051	-0.073	0.043	0.171	19
20	0.013	-0.068	0.045	0.059	0.026	-0.103	-0.040	-0.021	-0.064	-0.049	0.047	0.045	0.114	0.174	0.266	0.257	0.095	0.477	0.928	1.000	0.229	0.209	0.102	0.203	0.020	20
21	-0.394	-0.248	-0.328	-0.467	-0.518	-0.057	0.259	0.300	0.165	-0.227	-0.360	-0.440	-0.439	0.014	0.173	0.128	-0.061	-0.149	0.071	0.229	1.000	0.999	0.924	0.998	-0.372	21
22	-0.399	-0.251	-0.335	-0.470	-0.509	-0.049	0.259	0.303	0.169	-0.221	-0.358	-0.448	-0.450	0.005	0.161	0.118	-0.068	-0.163	0.051	0.209	0.999	1.000	0.926	0.999	-0.374	22
23	-0.403	-0.356	-0.387	-0.477	-0.449	0.175	0.440	0.473	0.336	-0.130	-0.305	-0.350	-0.420	0.022	0.132	0.037	-0.058	-0.181	-0.073	0.102	0.924	0.926	1.000	0.934	-0.299	23
24	-0.404	-0.274	-0.350	-0.481	-0.511	-0.033	0.260	0.307	0.179	-0.229	-0.362	-0.438	-0.448	-0.009	0.144	0.094	-0.081	-0.168	0.043	0.203	0.998	0.999	0.934	1.000	-0.382	24
25	0.765	0.561	0.802	0.890	0.707	0.293	0.304	0.263	0.400	0.721	0.777	0.757	0.624	-0.126	-0.277	-0.139	0.014	0.141	0.171	0.020	-0.372	-0.374	-0.299	-0.382	1.000	25

TABLE VI A

CORRELATION COEFFICIENTS FOR DATA OF....14 AUGUST AFTER SLICK

	1	2	3	4	5	6	7	8	9	10	11	12	13	14	15	16	17	18	19	20	21	22	23	24	25	
1	1.000	0.521	0.573	0.504	0.286	0.253	0.316	0.236	-0.056	0.066	0.259	-0.015	-0.091	0.210	0.399	0.393	0.122	-0.059	0.290	0.265	0.150	0.132	0.085	0.075	0.473	1
2	0.521	1.000	0.807	0.505	0.098	0.169	0.394	0.493	0.211	0.293	0.423	0.322	0.069	0.044	0.189	0.224	0.175	0.286	0.615	0.414	-0.055	-0.049	-0.080	-0.052	0.553	2
3	0.573	0.807	1.000	0.906	0.472	0.326	0.500	0.562	0.065	-0.039	0.229	0.189	-0.001	-0.022	0.236	0.263	0.083	0.227	0.497	0.272	-0.140	-0.150	-0.180	-0.132	0.764	3
4	0.504	0.505	0.906	1.000	0.651	0.368	0.474	0.516	-0.067	-0.268	0.026	0.040	0.002	0.014	0.250	0.190	-0.046	0.122	0.264	0.092	-0.154	-0.165	-0.186	-0.137	0.762	4
5	0.286	0.098	0.472	0.651	1.000	0.884	0.771	0.552	0.174	-0.210	0.054	0.113	-0.048	0.010	0.530	0.633	-0.021	-0.303	0.093	0.209	-0.290	-0.320	-0.320	-0.296	0.861	5
6	0.253	0.169	0.326	0.368	0.884	1.000	0.912	0.576	0.308	0.032	0.208	0.265	0.065	0.076	0.601	0.850	0.166	-0.308	0.186	0.315	-0.307	-0.341	-0.345	-0.330	0.840	6
7	0.316	0.394	0.500	0.474	0.771	0.912	1.000	0.766	0.247	0.067	0.184	0.228	0.258	0.269	0.624	0.795	0.180	-0.141	0.360	0.355	-0.464	-0.489	-0.504	-0.475	0.899	7
8	0.236	0.493	0.562	0.516	0.552	0.576	0.766	1.000	0.467	0.133	0.153	-0.022	0.093	0.449	0.655	0.476	-0.136	-0.065	0.548	0.457	-0.589	-0.579	-0.595	-0.589	0.758	8
9	-0.056	0.211	0.065	-0.067	0.174	0.308	0.247	0.467	1.000	0.708	0.464	0.234	-0.061	0.171	0.406	0.446	0.118	0.009	0.359	0.349	-0.073	-0.093	-0.067	-0.075	0.263	9
10	0.066	0.293	-0.039	-0.268	-0.210	0.032	0.067	0.133	0.708	1.000	0.742	0.566	0.330	0.163	0.139	0.277	0.457	0.335	0.115	0.027	0.218	0.175	0.188	0.221	0.033	10
11	0.259	0.423	0.229	0.026	0.054	0.208	0.184	0.153	0.464	0.742	1.000	0.824	0.025	-0.181	0.069	0.279	0.512	0.400	0.101	-0.019	0.385	0.346	0.333	0.339	0.280	11
12	-0.015	0.322	0.189	0.040	0.113	0.265	0.228	-0.022	0.234	0.566	0.824	1.000	0.314	-0.369	-0.212	0.209	0.627	0.515	-0.044	-0.243	0.331	0.287	0.287	0.330	0.278	12
13	-0.091	0.069	-0.001	0.002	-0.048	0.065	0.258	0.093	-0.061	0.330	0.025	0.314	1.000	0.457	0.041	0.085	0.195	0.244	-0.114	-0.408	-0.192	-0.209	-0.204	-0.106	0.100	13
14	0.210	0.044	-0.022	0.014	0.010	0.076	0.269	0.449	0.171	0.163	-0.181	-0.369	0.457	1.000	0.687	0.206	-0.317	-0.222	0.214	0.049	-0.305	-0.267	-0.277	-0.268	0.126	14
15	0.399	0.189	0.236	0.250	0.530	0.601	0.624	0.655	0.406	0.139	0.069	-0.212	0.041	0.687	1.000	0.660	-0.318	-0.504	0.319	0.330	-0.314	-0.308	-0.320	-0.303	0.570	15
16	0.393	0.224	0.263	0.190	0.633	0.850	0.795	0.476	0.446	0.277	0.279	0.209	0.085	0.206	0.660	1.000	0.325	-0.258	0.407	0.430	-0.269	-0.330	-0.342	-0.333	0.683	16
17	0.122	0.175	0.083	-0.046	-0.021	0.166	0.180	-0.136	0.118	0.457	0.512	0.627	0.195	-0.317	-0.318	0.325	1.000	0.670	0.075	0.003	0.327	0.247	0.244	0.247	0.142	17
18	-0.059	0.286	0.227	0.122	-0.303	-0.308	-0.141	-0.065	0.009	0.335	0.400	0.515	0.244	-0.222	-0.504	-0.258	0.670	1.000	0.135	-0.226	0.310	0.284	0.283	0.310	-0.047	18
19	0.290	0.615	0.497	0.264	0.093	0.186	0.360	0.548	0.359	0.115	0.101	-0.044	-0.114	0.214	0.319	0.407	0.075	0.135	1.000	0.729	-0.482	-0.473	-0.492	-0.527	0.386	19
20	0.265	0.414	0.272	0.092	0.209	0.315	0.355	0.457	0.349	0.027	-0.019	-0.243	-0.408	0.049	0.330	0.430	0.003	-0.226	0.729	1.000	-0.490	-0.476	-0.473	-0.538	0.342	20
21	0.150	-0.055	-0.140	-0.154	-0.290	-0.307	-0.464	-0.589	-0.073	0.218	0.385	0.331	-0.192	-0.305	-0.314	-0.269	0.327	0.310	-0.482	-0.490	1.000	0.991	0.987	0.977	-0.305	21
22	0.132	-0.049	-0.150	-0.165	-0.320	-0.341	-0.489	-0.579	-0.093	0.175	0.346	0.287	-0.209	-0.267	-0.308	-0.330	0.247	0.284	-0.473	-0.476	0.991	1.000	0.997	0.979	-0.331	22
23	0.085	-0.080	-0.180	-0.186	-0.320	-0.345	-0.504	-0.595	-0.067	0.188	0.333	0.287	-0.204	-0.277	-0.320	-0.342	0.244	0.283	-0.492	-0.473	0.987	0.997	1.000	0.985	-0.349	23
24	0.075	-0.052	-0.132	-0.137	-0.296	-0.330	-0.475	-0.589	-0.075	0.221	0.339	0.330	-0.106	-0.268	-0.303	-0.333	0.247	0.310	-0.527	-0.538	0.977	0.979	0.985	1.000	-0.311	24
25	0.473	0.553	0.764	0.762	0.861	0.840	0.899	0.758	0.263	0.033	0.280	0.278	0.100	0.126	0.570	0.683	0.142	-0.047	0.386	0.342	-0.305	-0.331	-0.349	-0.311	1.000	25

Bibliography

Barber, N.F.,1963, The directional resolving power of an array of wave detectors, in Ocean Wave Spectra, Englewood Cliffs, N. Y., Prenctice-Hall, Inc., pp 137-150.

Bendat, J. A. and A. G. Piersol, 1966, Measurement and analysis of random data, New York, John Wiley & Sons, Inc.

Ford, J. R., R. C. Timme and A. Trampus, 1967, A new method for obtaining the directional spectrum of ocean surface gravity waves in marine technology society, The New Thrust Seaward, Washington, D. C., Marine Technology Society.

Gilchrist, A. W. R., 1966, The directional spectrum of ocean waves: an experimental investigation of certain predictions of the Miles - Phillips theory of wave generation, J. Fluid Mech., 25, pp 795-816.

Goodman, N. R., 1957, Statistical analysis based on a certain multivariate complex gaussian distribution (An Introduction) Ann. of Math. Statistics, 34, pp 152-177.

Hasselman, K. W., Munk, G. Mac Donal, 1963, Bispectra of ocean waves in Symposium on time series analysis, Brown University, 1962, New York, John Wiley & Sons, Inc., pp 125-139.

Hoel, P. G., 1962, Introduction to mathematical statistics (3rd ed.) New York, John Wiley & Sons, Inc.

Kinsman, B., 1965, Wind Waves, Englewood Cliffs, New York, Prentice-Hall, Inc.

Lamb, H., 1945, Hydrodynamics (6th ed.) London, Cambridge, University Press, (New York, reprinted by Dover Publ., Ind., 1945.)

Lighthill, M. J., 1962, Physical interpretation of the mathematical theory of wave generation by wind, J. Fluid Mech., 14, (3) pp. 385-398.

Longuet-Higgins, M.S., D.E. Cartwright, and N.D. Smith, 1963, Observations of the directional spectrum of sea waves using the motions of a floating buoy, Ocean Waves Spectra, Englewood Cliffs, New York, Prentice-Hall Inc., pp 111-132.

and R. W. Stewart, 1969, Changes in the form of short gravity waves on long waves and tidal currents, J. Fluid Mech., 8, (4), pp 565-581.

Miles, J. W., 1957, On the generation of surface waves by shear flow, J. Fluid Mech., 3 (2) pp. 185-204.

1959, On the generation of surface flows by shear flows Part 2, J. Fluid Mech., 6 (4) pp. 568-582.

1960, On the generation of surface waves by turbulent shear flows Part 3, J. Fluid Mech., 7 (3) pp. 469-478.

1962, On the generation of surface waves by turbulent shear flows Part 4, J. Fluid Mech., 13 (3) pp. 433-448.

Munk, W. H., G. R. Miller, F.E. Snodgrass and N.F. Barber, 1963, Directional recording of swell from distant storms, Phil, Trans. A., 255, 505-584.

Phillips, O.N., 1957, On the generation of waves by turbulent wind, J. Fluid Mech., 2 (5) 417-445.

1958, The equilibrium range in the spectrum of wind generated waves, J. Fluid Mech., 4 (4) 426-434.

1966, The dynamics of the upper ocean, London, Cambridge University Press.

and E. J. Katz, 1961, The low frequency components of the spectrum of wind generated waves, J. Mar. Res., 19 (2) pp. 57-69.

Ruggles, K. W., 1969, Observations of the wind field in the first ten meters of the atmosphere above the ocean, Mass. Inst. of Tech., Dept. of Meteor., Technical report.

Seesholtz, J. R., 1968, A field investigation of air flow immediately above the ocean surface waves, Mass. Inst. of Tech., Dept of Meteor., Technical report.

Shonting, D. H., 1966, Observations of particle motions in ocean waves, Sc.D. Thesis, Mass. Inst. of Tech., Dept of Meteor.

Witham, G. B., 1960, A note on group velocity, J. Fluid Mech., 9 pp 347-52.

Acknowledgements

The author would like to thank Professor Erik Mollo-Christensen for his long and incessant support of this investigation.

Thanks also go to Messrs Peers and Morey for their large amount of time and effort invested in setting up the experiments and in analysing the results.

Cmdrs K. W. Ruggles and J. R. Seesholtz, USN, were extremly helpful as good friends and critical judges of many ideas used in this work.

Biography

Ortwin H. von Zweck was born in Bernburg, Germany on 24 November 1938. In 1947 his family moved to Austria where he attended public school, from 1955 to 1958 he attended high school in Campbellford, Ontario.

In 1963 he obtained his BA and in 1965 his M.S. in Physics from Northeastern University in Boston, Massachusetts. Since 1965, when he first began his studies at M.I.T, he became an U.S. citizen and married the former Ann Place Smith.